TEM analysis of “Communitymasker M-VYG-A1” mouth masks

	Recipient of the report	Realised by
Name	**This work was realized in the framework of the AgMask project**	**x**
E-mail		**x**
Telephone		x
Organization		Sciensano
Address		x
Zip Code		x
City		Brussels
Country		Belgium
Other contacts		

Contents

Background information 3

Goal 3

Experimental methodology 3

Materials 3

Methodology 4

Sample Preparation 4

Microscope alignment and calibration 5

Descriptive EM analysis 5

EDX analysis 6

Results 7

Descriptive EM analysis 7

EDX analysis 8

Conclusions 8

Figures 10

F.1 Sample T14D: external layer, repetition 1 10

F.2 Sample T14E: Middle layer, repetition 1 12

F.3 Sample T14F: internal layer, repetition 1 14

F.4 Sample T14G: External layer, repetition 2 19

F.5 Sample T14H: Middle layer, repetition 2 20

F.6 Sample T14I: Internal layer, repetition 2 26

F.7 Sample T17A: External layer, repetition 3 33

F.8 Sample T17B: Middle layer, repetition 3 34

F.9 Sample T17C: Internal layer, repetition 3 37

References 47

Background information

Treatment of textiles with silver based biocides gives the textiles a broad spectrum antibacterial and antiviral properties. Many types of mouth masks offered on the Belgian market and online are also treated with silver. The use of silver in mouth masks is accompanied by safety concerns as to whether silver ions or nanoparticles may be released, and depends on the type of silver based biocide (ionic or particulate), its stability during application and cleaning, and the type of exposure of the users.
In the AgMask project, the application of silver based biocides and/or of other nanoparticles in mouth masks available on the Belgian market is evaluated. This report summarizes the results of the TEM based analyses performed on "Communitymasker M-VYG-A1" mouth masks, obtained in the context of the AgMask project.

Goal

The goal is to evaluate the presence of silver (Ag) based biocides and/or of other nanoparticles *in situ*, in the "Communitymasker M-VYG-A1" mouth masks by conventional and analytical TEM. The applied sample preparation, TEM imaging and analysis aim to identify and measure the size, shape, agglomeration state and elemental composition of the nanoparticles in sections of the mouth masks. It is assessed wether nanoparticles are completely embedded in the textile fibers or if they are applied as an external coating. This is an important factor to predict wether migration of nanoparticles may occur.
The applied TEM based methods are described in detail in the book chapters of Mast et al.[1], and applied and validated for the analyses of nanoparticles in the publication of Verleysen et al.[2]
It should be noted that washing or abrazion of the mouth masks might significantly influence the release of nanoparticles. This issue is considered out of scope for this report. It will be considered in work package 3 of the AgMask project.

Experimental methodology

Materials

Figure 1 shows the information file that was present in the packaging of the mouth masks. The mouth masks were produced by "Viet y - hung yen garment joint stock company" and imported by "Avrox".
The mouth masks consist of three layers (external, middle, internal), with the internal layer being closest to the mouth when worn. The three layers are analysed individually, and three replicates of each layer were analysed. According to the information file shown in Figure 1, one layer consists 100% of polyester, and the two other layers consist of a mixture of 65% polyester and 35% coton. Information about the samples is provided in Table 1.

Table 1 General overview of the samples

Sciensano's Reference	Sample description	Number of analysed sections	Evaluation of sample preparation by BF-TEM	Type of fiber observed by TEM
T14D	External layer, repetition 1	1	Ok	polyester
T14E	Middle layer, repetition 1	1	Ok	polyester + coton
T14F	Internal layer, repetition 1	4	Ok	polyester + coton
T14G	External layer, repetition 2	3	Ok	polyester
T14H	Middle layer, repetition 2	2	Ok	polyester + coton
T14I	Internal layer, repetition 2	1	Ok	polyester + coton
T17A	External layer, repetition 3	1	Ok	polyester
T17B	Middle layer, repetition 3	1	Ok	polyester + coton
T17C	Internal layer, repetition 3	1	Ok	polyester + coton

Figure 1 Information file that was present in the packaging of the mouth masks

Methodology

Sample Preparation

A methodology based on the procedure described by Gashti et al.[3] is followed, where ultra-thin sections of textiles are prepared by embedding them in an epoxy resin, followed by ultra-thin sectioning using ultramicrotomy. The ultra-thin sectioning sample preparation is realized as described in the Sciensano SOP entitled: "Ultra-thin sectioning for transmission electron microscopy".

The sample preparation protocol for nanoparticles in textiles includes:

- Cutting a piece of the textile sample of about 1 cm long and 0.5 cm wide.
- Embedding the textile sample in Epon medium (EPON812-Spurr resin mixture: This mixture is obtained by mixing equal amounts (usually 50 ml) of Spurr and EPON812 solutions. Spurr is prepared by dissolving 13.3 g vinyl cyclohexene dioxide (VCD, Agar Scientific Ltd., ERL4206), 7 g DER736 (Fluka, 31191), 34.7 g 2-nonen-1-ylsuccinic anhydride (NSA, Fluka, 74378) and 0.53 g 2-dimethylamino ethanol (DMAE, Fluka, 38990) in 50 ml of distilled water. EPON is obtained by mixing 27.3 g EPON 812 (Fluka 45345), 10.8 g 2-dodecen-1- ylsuccinic anhydride (DDSA, Fluka, 44161), 18.7 g methylnorbornene-2,3-dicarboxylic-acid (MNA, Fluka, 68165) and 0.9 g 2,4,6-Tris(dimethyl-aminomethyl)phenol (DMP30, Fluka, 93331) with 50 ml distilled water) and heating overnight at 70°C.
- Trimming specimen blocks with an Ultracut ultramicrotome with TM60 trimming unit (Reichert-Jung A.G., Vienna, Austria) to obtain a cutting face of 0.5 - 1 mm^2 to 1 - 2 mm^2.
- Cutting ultrathin sections in the yellow to green interference color range, corresponding with a section thickness between 60-250 nm
- Bringing the sections on pioloform-coated 200 mesh copper grids.

Microscope alignment and calibration

Suitable alignment of the microscope is a prerequisite to reach optimal lens conditions for TEM imaging, and is daily evaluated, following the tutorials of Rodenburg et al.[4] and Williams and Carter[5].
To assure the precision and accuracy of TEM measurements and to relate them to the international system of units (SI), calibration of the TEM is critical. This is realized supporting on the guidance document ISO29301[6] for magnification calibration of the images over the applied magnification range.
Calibration is done at two levels. Firstly, the reference materials applied for magnification calibration possess a periodic structure that makes it suitable for automated calibration using the specialized calibration software, according to the manufacturer's instructions. In a second step, a complementary evaluation based on measurement of the size of a certified reference materials with an SI-traceable size is foreseen periodically.
Images were recorded using the conditions described in Table 2.

Descriptive EM analysis

Before other analyses are initiated, a detailed description of the material present on the TEM grid is a first and essential step to assess the quality of the sample preparation, and to determine the properties of the examined nano-objects. Based on a series of representative images recorded at high, intermediate and low magnifications, and covering the entire specimen, an overview of the specimen is given and the properties of the nano-objects of interest such as size, morphology, and agglomeration state, are visualized in the electron microscope. The proposed methodology complies with the EFSA Guidance documents [7,8] that foresee application of EM. It describes key parameters important to assess the nanomaterial safety as specified in [8–11]. The descriptive EM analysis includes at least (i) an estimate of the size (distribution) of the constituent and aggregated/agglomerated particles, (ii) representative and calibrated micrographs; (iii) the agglomeration- and aggregation status; (iv) the general morphology; (v) the surface topology; (vi) the structure (crystalline, amorphous, …); and (vii) the presence of contaminants and aberrant particles.
In addition, descriptive EM analysis reports the specimen quality including possible impurities, large agglomerates, deformations and artefacts, and the homogeneity of the material on the grid. Supporting on these parameters, the relevance and suitability of an elemental analysis and/or quantitative EM is evaluated.
To categorize and describe the surface structure, the particle shape, and the shape of aggregates and agglomerates, the systems proposed by, respectively, Krumbein and Sloss[12], Munoz-Marmol[13], and Lopeze-de-Uralde[14] are applied.
Figure 2 is applied for systematic reporting of the results of descriptive EM analysis. This systematic approach reduces errors and assures uniformity in reporting by suggesting possible descriptions in drop lists.

Transmission electron micrographs are recorded using the TEM imaging & analysis (TIA) software (Thermo Fischer Scientific, Eindhoven, The Netherlands). These SER- and EMI- formatted micrographs were converted to TIF format using the TIA software. For BF-TEM imaging, the condenser lens current is chosen such that the beam is parallel and images are taken approximately 500 nm below minimal contrast conditions, where Fresnel fringes are minimal and contrast is judged to be optimal. The specific TEM imaging conditions are summarized in Table 2.

STEM images were recorded using the Velox software (Thermo Fischer Scientific, Eindhoven, The Netherlands). The resulting .emd formatted micrographs were converted to TIF ang JPG format using the Velox software. In STEM imaging, a convergent beam is scanned across the specimen surface. The electrons scattered at high angle are detected using a high angle annular dark field (HAADF) detector, and are used to form an image. The intensity in a HAADF-STEM image is proportional to the specimen thickness and (approximately) to the squared atomic number. The specific STEM imaging conditions are summarized in Table 2.

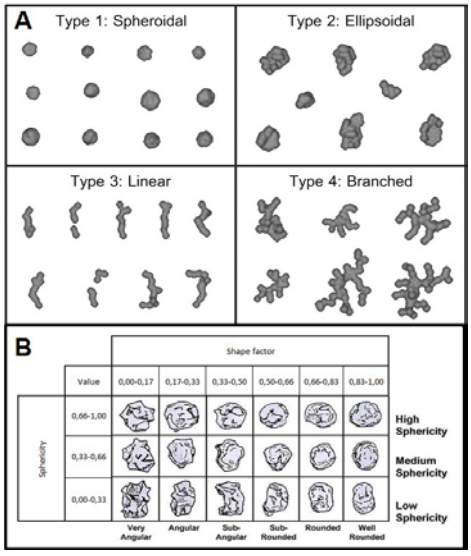

Figure 2 Description of the shape (A), and surface topology (B) (sphericity and shape factor) of constituent particles and aggregates/agglomerates.

EDX analysis

EDX analysis is performed on the EM specimens to determine the elemental composition of the particles of interest. The specimens are analysed by a Super-X EDS detector (ThermoFisher, Eindhoven, The Netherlands) consisting of 2 windowless silicon drift detectors (SDD). Analysis results include spectral images and spectra. Specific EDX analysis conditions are summarized in Table 2.

Table 2 Summary of the EM imaging and analysis conditions.

EM imaging conditions	TEM	STEM	EDX
Type of microscope	Tecnai Spirit 12	Talos F200S	Talos F200S
Type of analysis	TEM	STEM	STEM-EDX
Voltage	120 kV	200 kV	200 kV
Detection system	Bottom-mounted 4X4K Eagle CCD camera	HAADF detector	Super-X EDS detector
Spot size	3	x	x
Emission step	2	Not relevant	Not relevant
Convergence angle (mrad)	Parallel beam conditions	x	x
Screen current (nA)		x	x
Scan size	4096 x 4096	1024 x 1024	1024 x 1024
Dwell time	Not relevant	x	x
Auto Stop	Not relevant	Not relevant	5 or 10 frames
Live time (min)	Not relevant	Not relevant	2.1 or 4.2
Gain (%)	Not relevant	Optimized per image	Optimized per image
Offset (%)	Not relevant	Optimized per image	Optimized per image
Camera length of detector	Not relevant	x	x
Energy range (keV)	Not relevant	x	x
Date of the last maintenance	16/11/2020	20/11/2020	20/11/2020
Date of the last calibration	16/11/2020	20/11/2020	20/11/2020
Size calibration method	the cross-grating method based on a 2160 lines/mm optical diffraction-cross grating	the cross-grating method based on a 2160 lines/mm optical diffraction-cross grating	Not relevant

Results

Descriptive EM analysis

Before further analysis, the quality of the sample preparation was verified by BF-TEM. In all samples, textile fibers were detected in the sections (Table 1). In all samples, sample preparation artefacts caused by cutting and compression were minimal.

The samples are described in detail based on representative and selected electron micrographs obtained by HAADF-STEM (Figures parts F.1-F.9). Table 3 indicates for each sample the corresponding collection of figures (F1 – F9).
The selected imaging conditions allowed analyzing the sections at high resolution while transferring only a limited dose (current of 0.02nA), avoiding beam induced damage.

In the three repetitions of the external layer, i.e. samples T14D, T14G and T17A, only one type of fiber was detected. This is in agreement with the description in the information file (Figure 1) which states that the masks contain 1 layer that consists 100% of polyester.
The polyester fibers show circular cross sections and contain particles with medium sphericity (near-spherical) in the size range of 50 to 250 nm. This is shown in Figure 3, Figure 15, and Figure 35 for samples T14D, T14G and T17A, respectively. The particles were agglomerated. The agglomerates were ellipsoidal, had a size ranging from 100 to 500 nm and consisted of about 2 to 100 constituent particles (Figure 3, Figure 15, Figure 35). The particles in the polyester fibers were mainly localized inside the fibers, although certain particles were observed at the edge of the fibers (Figure 3, Figure 15, Figure 35).

The three repetitions of the middle layer (T14E, T14H and T17B) and the 3 repetitions of the internal layer (T14F, T14I and T17C) showed similar results: in all samples two types of fibers were detected. This is shown in Figure 6, Figure 8, Figure 18, Figure 26, Figure 37, and Figure 41 for samples T14E, T14F, T14H, T14I, T17B and T17C, respectively. This finding is in agreement with the description given in the information file (Figure 1) which states that the masks contain 2 layers that contain 65% polyester and 35% coton.
The polyester fibers show circular cross sections and contain particles with medium sphericity (near-spherical) in the size range of 50 to 250 nm (Figure 6, Figure 8, Figure 18, Figure 19, Figure 26, Figure 27, Figure 37, and Figure 41). The particles were agglomerated. The agglomerates were ellipsoidal, had a size ranging from 100 to 500 nm and consisted of about 2 to 100 constituent particles.
The particles in the polyester fibers were mainly localized inside the fibers, although certain particles were observed at the edge of the fibers. This is shown in Figure 6, Figure 13, Figure 19 and Figure 29A for samples T14E, T14F, T14H and T14I, respectively.
The coton fibers show a void or thinner region in the center (Figure 6, Figure 8, Figure 18, Figure 26, Figure 37, and Figure 41). Particles are detected at the edge of some of the coton fibers in samples T14E (Figure 6), T14F (Figure 10, Figure 12, and Figure 14), T14H (Figure 21, Figure 22, Figure 23, Figure 24, and Figure 25), T14I (Figure 32, and Figure 34), T17B (Figure 39 and Figure 40) and T17C (Figure 43, Figure 44, Figure 45, Figure 46, Figure 47, Figure 48, Figure 49 and Figure 50). The observed individual and agglomerated particles were near-spherical and ranged from 10 nm to 150 nm in diameter.

A significant amount of particles was detected outside of the textile fibers (e.g. Figure 11, Figure 30, Figure 31). It needs to be further examined wether these particles were released from the fibers or if they originate from a sample preparation artefact caused by slicing the textile fibers using a diamond knife.

EDX analysis

Table 3 summarizes the EDX results for each sample. EDX analysis showed that all polyester fibers contain TiO_2 particles, which are generally located inside the fibers (Figure 4, Figure 7, Figure 9, Figure 16, Figure 20, Figure 28, Figure 36, Figure 38, and Figure 42), but also at the edge of the fibers (Figure 5, Figure 13, Figure 17, and Figure 29). TiO_2 particles are sometimes found outside of the textile fibers but inside of the section (Figure 11, Figure 30 ,Figure 31). In samples T14F, T14H, T14I, T17B and T17C, TiO_2 particles were detected at the edge of the coton fibers (Figure 10, Figure 21, Figure 32, Figure 33, Figure 39, Figure 43, and Figure 44).

EDX analysis showed that Ag nanoparticles were present at the edge of some of the sections of coton fibers in samples T14F (Figure 12 and Figure 14), T14H (Figure 22, Figure 23, Figure 24, and Figure 25), T14I (Figure 32, Figure 33, and Figure 34), T17B (Figure 40) and T17C (Figure 44, Figure 46, Figure 47, Figure 48, Figure 49, and Figure 50). In addition, an iron oxide particle was detected at the edge of a coton fiber in sample T17C (Figure 45).

Because the examined ultrathin sections are approximately 120 nm – 150 nm thick, while the fibers are much longer, the finding of particles on (several of) these sections indicates that the entire length of the fiber is covered with particles.

Conclusions

The mouth masks contain an external layer consisting of polyester, and a middle and internal layer consisting of a combination of polyester and coton.
All polyester fibers contain agglomerated TiO_2 particles. Most TiO_2 particles are situated inside the fibers, although a significant fraction is located at the edge of the fibers. Some TiO_2 particles are found outside of the fibers and at the edge of the coton fibers. It is possible that these particles were released due to friction caused by sectioning the fibers using a diamond knife. This observation urges to examine if particles can be released while using the mouthmask under conditions of normal use (work package 2 of the AgMask project) and under abrazion conditions (work package 3).

Some of the coton fibers show silver particles at the edge of the fibers. The ultra thin sections have a thickness of approximately 120 nm – 150 nm. Because sections of fibers were readily found where one or several silver particles were observed, it can be assumed that the entire length of the fiber is covered with particles.

An relevant technical side note is that illumination of silver ions with a highly energetic electron beam can result in the artificial *de novo* synthesis of metallic silver particles from silver ions. In this case, this scenario seems unlikely because no expected growth from small to larger particles is observed, as shown earlier in experiment T13. Moreover, the observed silver nanoparticles are situated only at the outside of the fibers as expected for coating of fibers with nanoparticles. This will be examined in more detail.

Table 3 Summary of results obtained by qualitative STEM analysis and STEM-EDX analysis.

Sciensano's Reference	Sample description	Images for qualitative analyses shown in figure section	Type of fiber observed by TEM	Particles detected by EDX in polyester fibers	Particles detected by EDX on the edge of coton fibers
T14D	External layer, repetition 1	F.1	polyester	TiO_2	No coton fibers
T14E	Middle layer, repetition 1	F.2	polyester + coton	TiO_2	No particles measured by EDX
T14F	Internal layer, repetition 1	F.3	polyester + coton	TiO_2	Ag, TiO_2
T14G	External layer, repetition 2	F.4	polyester	TiO_2	No coton fibers
T14H	Middle layer, repetition 2	F.5	polyester + coton	TiO_2	Ag, TiO_2
T14I	Internal layer, repetition 2	F.6	polyester + coton	TiO_2	Ag, TiO_2
T17A	External layer, repetition 3	F.7	polyester	TiO_2	No coton fibers
T17B	Middle layer, repetition 3	F.8	polyester + coton	TiO_2	Ag, TiO_2
T17C	Internal layer, repetition 3	F.9	polyester + coton	TiO_2	Ag, TiO_2, FeO,

Figures

F.1 Sample T14D: External layer, repetition 1

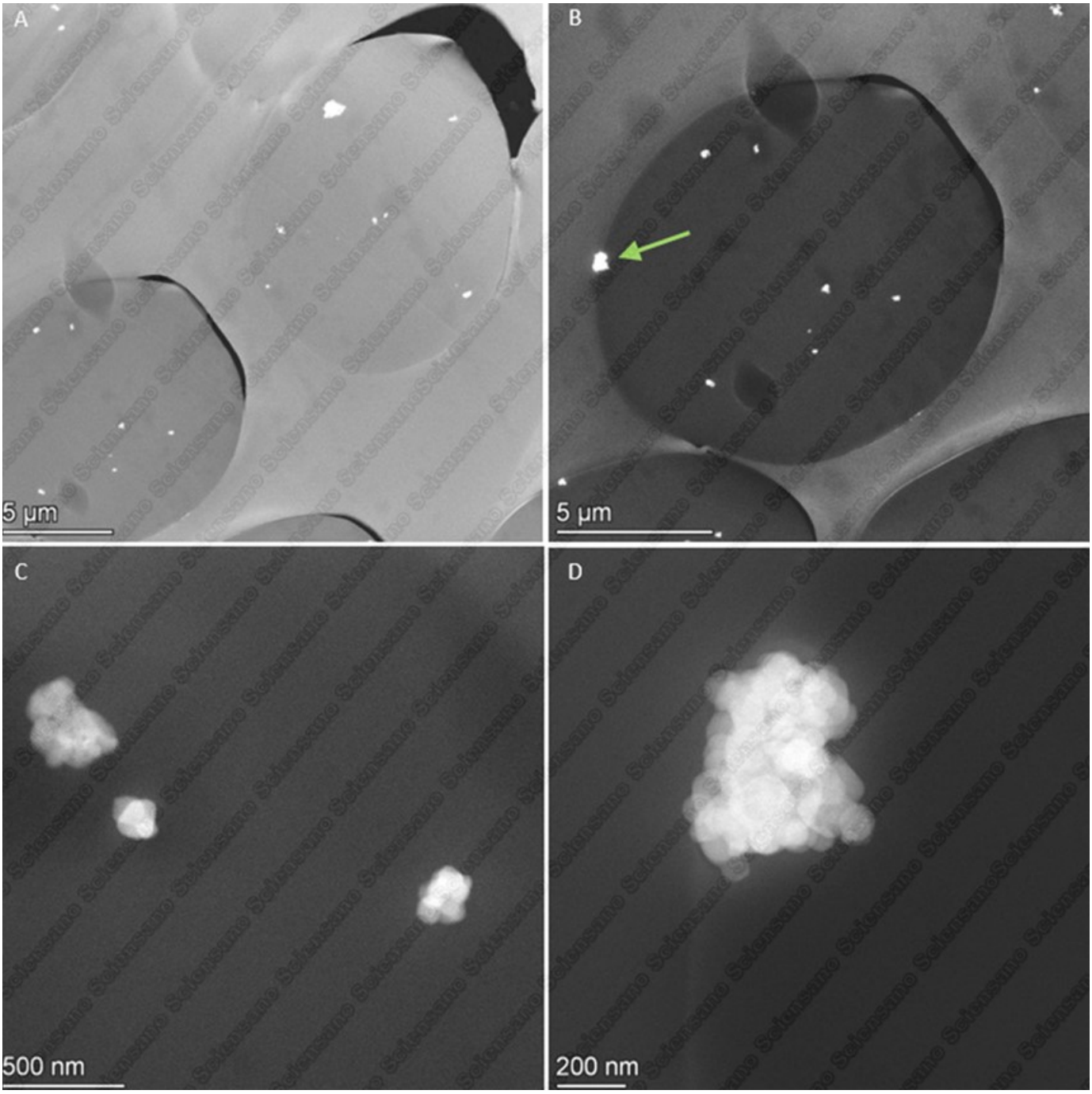

Figure 3 Representative HAADF-STEM images of sample T14D showing agglomerated near-spherical particles in cross sections of polyester fibers at low (A, B) and high (C,D) magnifications. The agglomerate shown in figure D lies at the edge of the fiber shown in B (arrow).

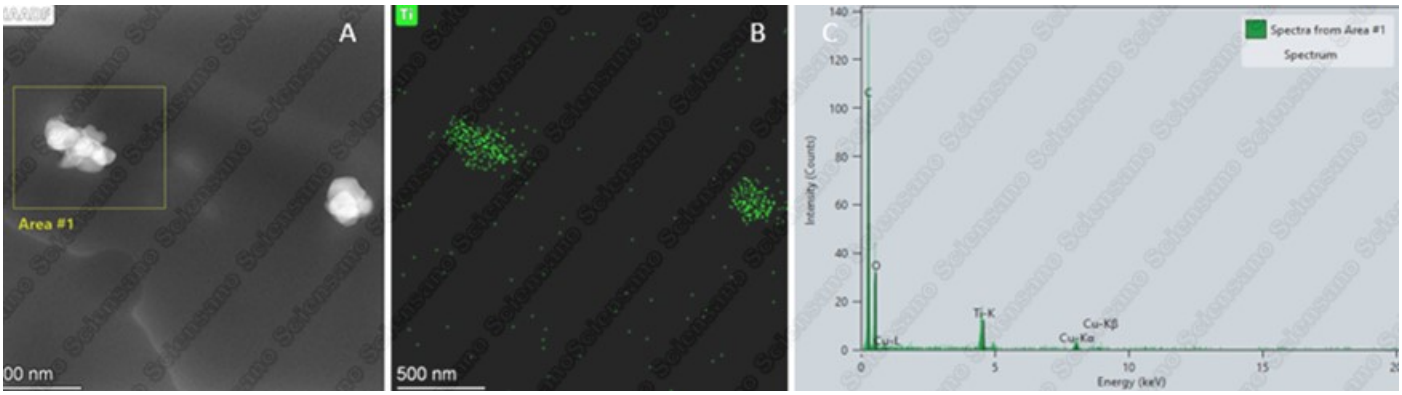

Figure 4 (A) HAADF-STEM image after analysis combined with (B) EDX spectral image of Ti and (C) EDX spectrum of the area indicated in A, demonstating that the particles found in the fibers of sample T14D are TiO_2 particles.

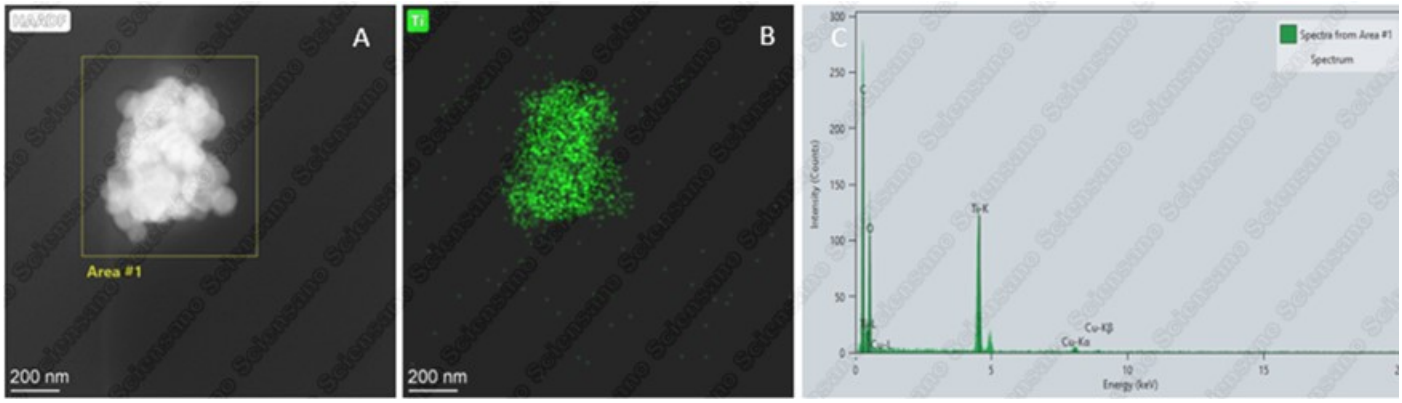

Figure 5 (A) HAADF-STEM image after analysis combined with (B) EDX spectral image of Ti and (C) EDX spectrum of the area indicated in A, demonstating that the agglomerate at the edge of a fiber shown in Figure 3D consists of TiO_2 particles.

F.2 Sample T14E: Middle layer, repetition 1

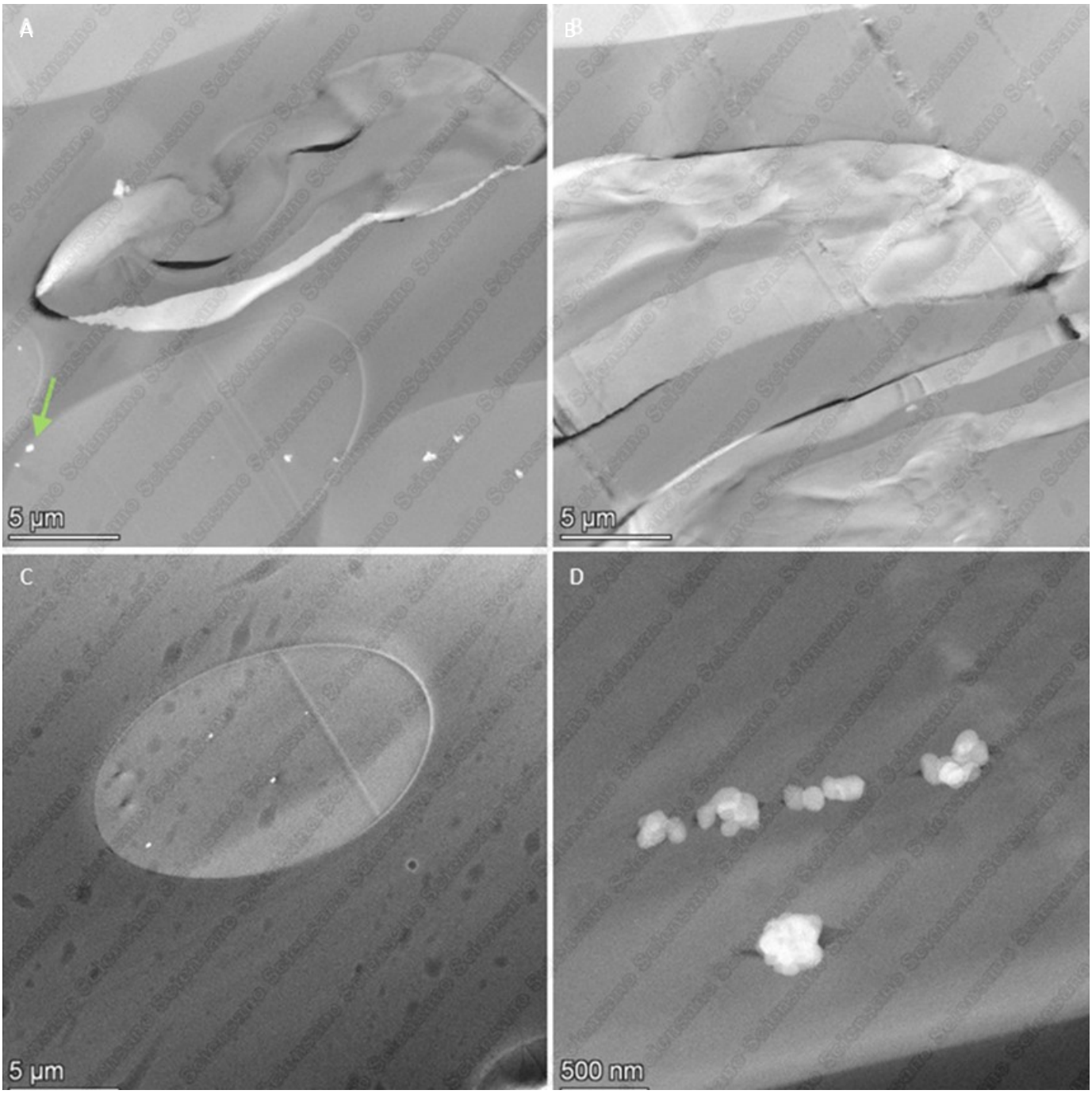

Figure 6 Representative HAADF-STEM images of sample T14E showing (A) two types of fibers present in the sample: (B) coton fibers showing a void or thinner region in the center, and (C, D) polyester fibers containing agglomerated near-spherical particles at low (C) and high (D) magnifications. Particles are generally located inside the fibers, although some particles are found at the edge of the fibers (green arrow).

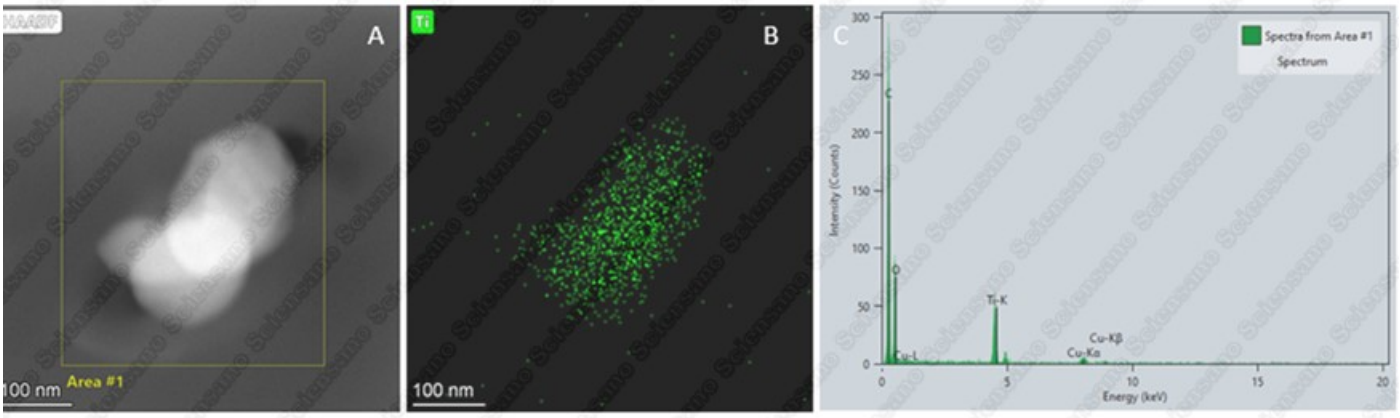

Figure 7 (A) HAADF-STEM image after analysis combined with (B) EDX spectral image of Ti and (C) EDX spectrum of the area indicated in A, demonstating that the particles found in the polyester fibers of sample T14E are TiO_2 particles.

F.3 Sample T14F: Internal layer, repetition 1

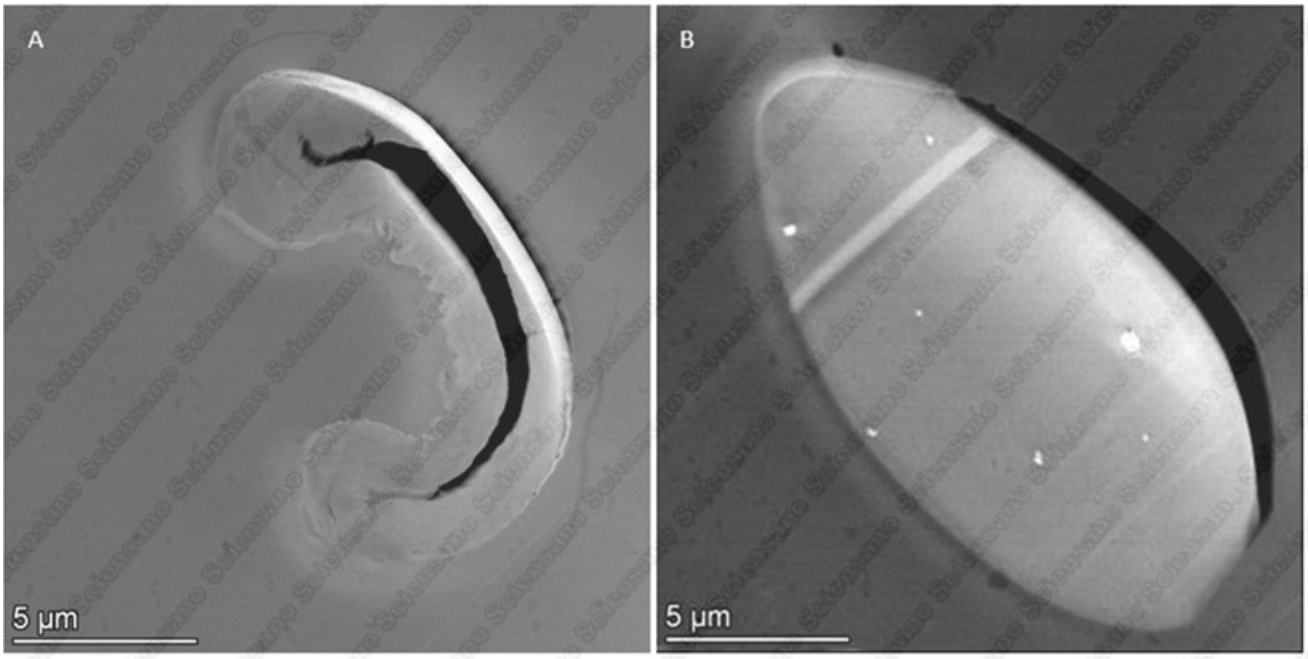

Figure 8 Representative HAADF-STEM images of sample T14F, showing two types of fibers present in the sample: (A) a coton fiber showing a void or thinner region in the center and (B) a polyester fiber containing agglomerated near-spherical particles.

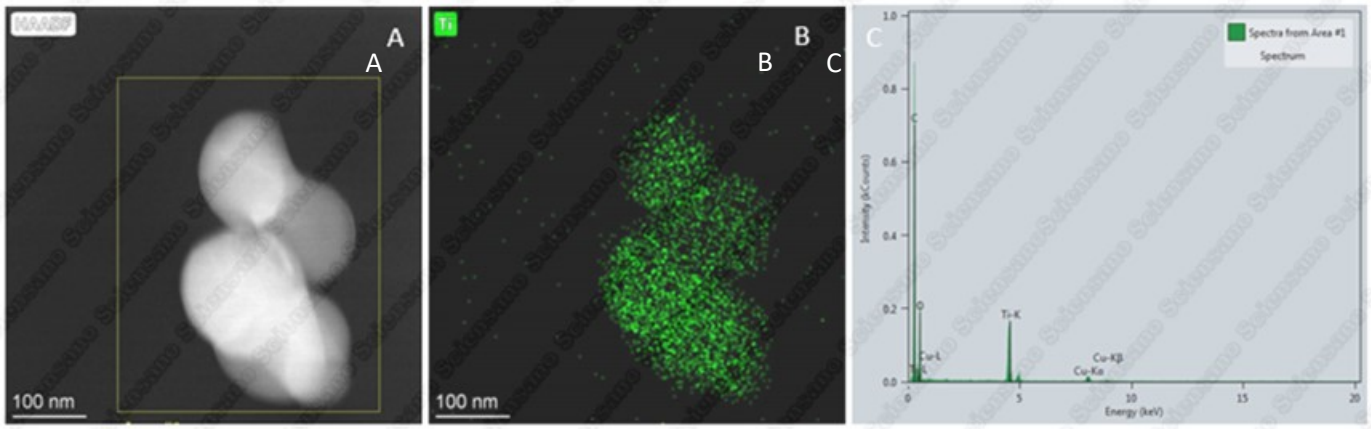

Figure 9 (A) HAADF-STEM image after analysis combined with (B) EDX spectral image of Ti and (C) EDX spectrum of the area indicated in A, demonstating that the particles found in the polyester fibers of sample T14F are TiO_2 particles.

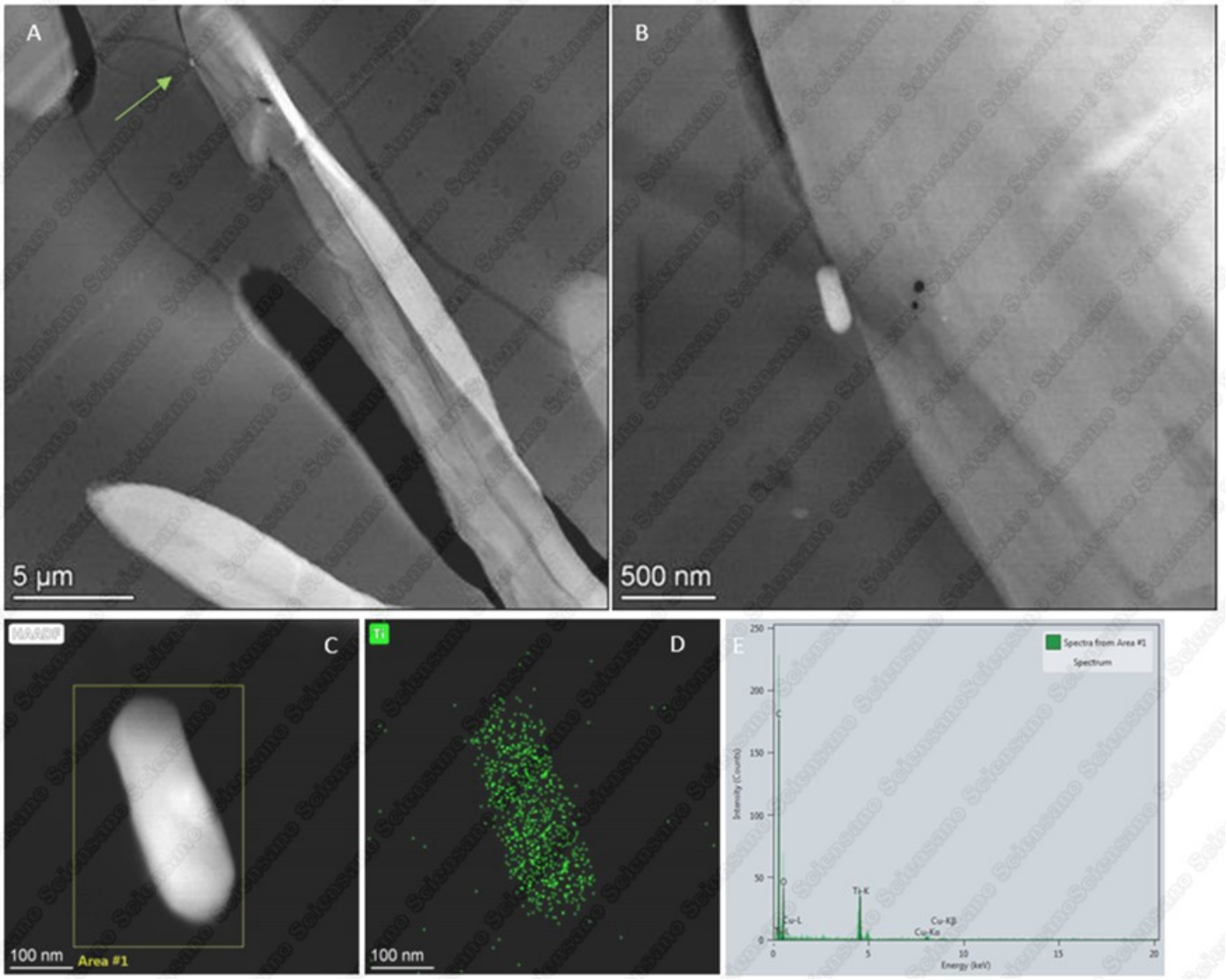

Figure 10 selected HAADF- STEM images at (A) low and (B) intermediate magnification, showing a particle at the edge of a coton fiber and corresponding EDX results with (C) the STEM image after analysis, (D) the spectral image of Ti, and (E) the spectrum of the region indicated in C.

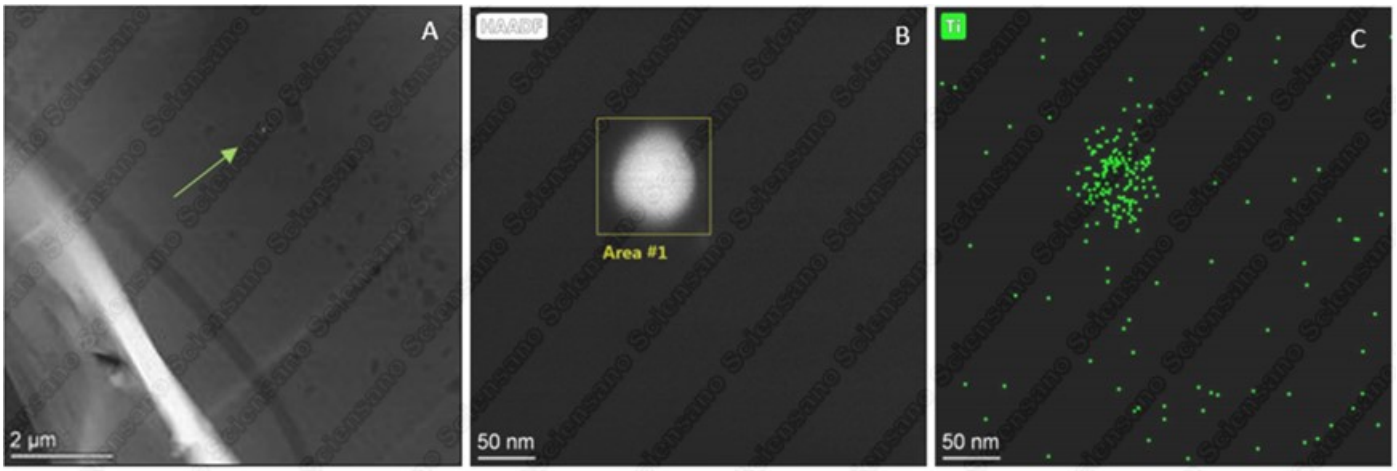

Figure 11 (A) selected HAADF- STEM image showing a particle which is not attached to a fiber (arrow), and corresponding EDX results with (B) the STEM image after analysis, and (C) the spectral image of Ti.

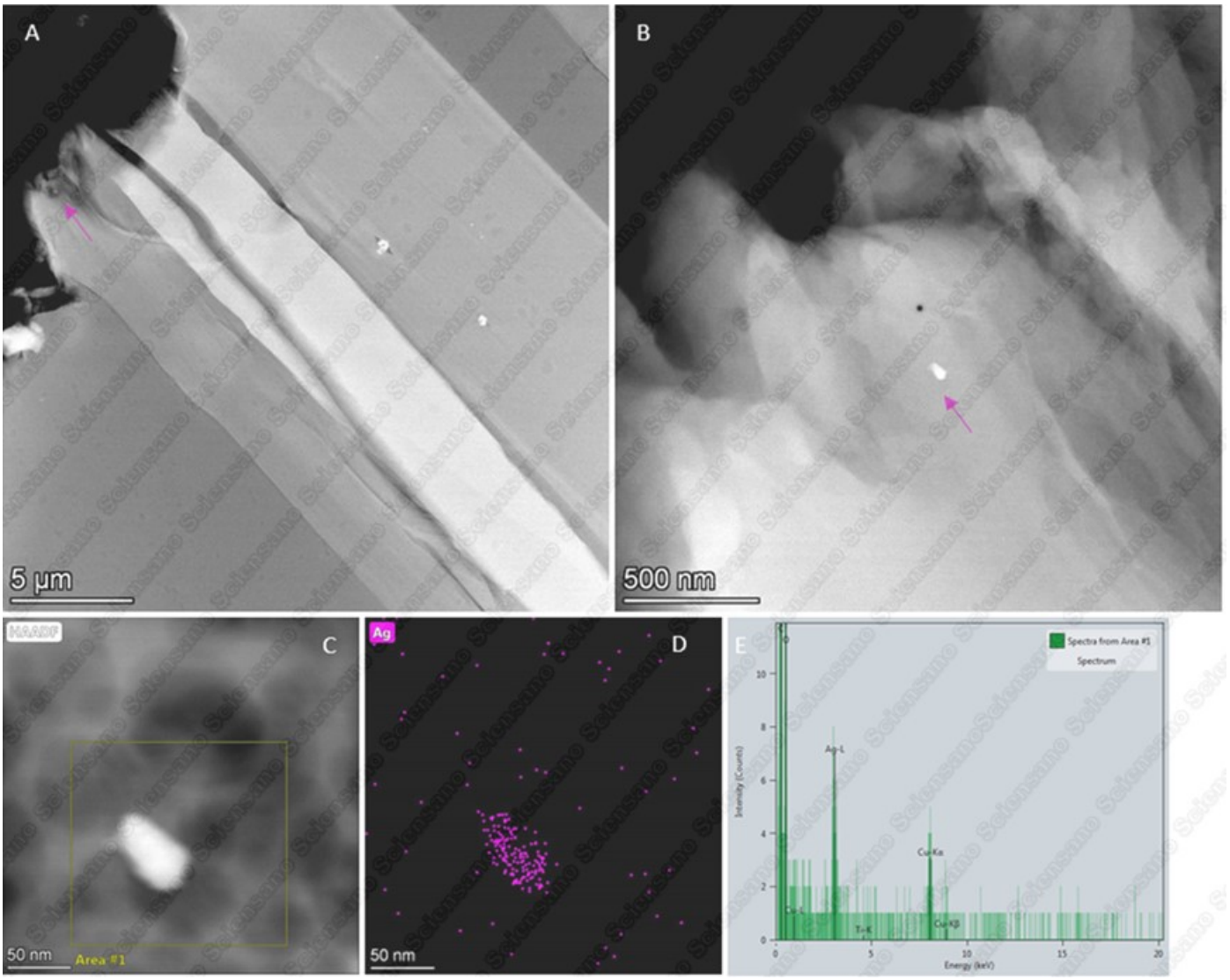

Figure 12 selected HAADF- STEM images at (A) low and (B) intermediate magnification, showing a particle on a coton fiber at the end of the section (arrow), and corresponding EDX results with (C) the STEM image after analysis, (D) the spectral image of Ag, and (E) the spectrum of the region indicated in C.

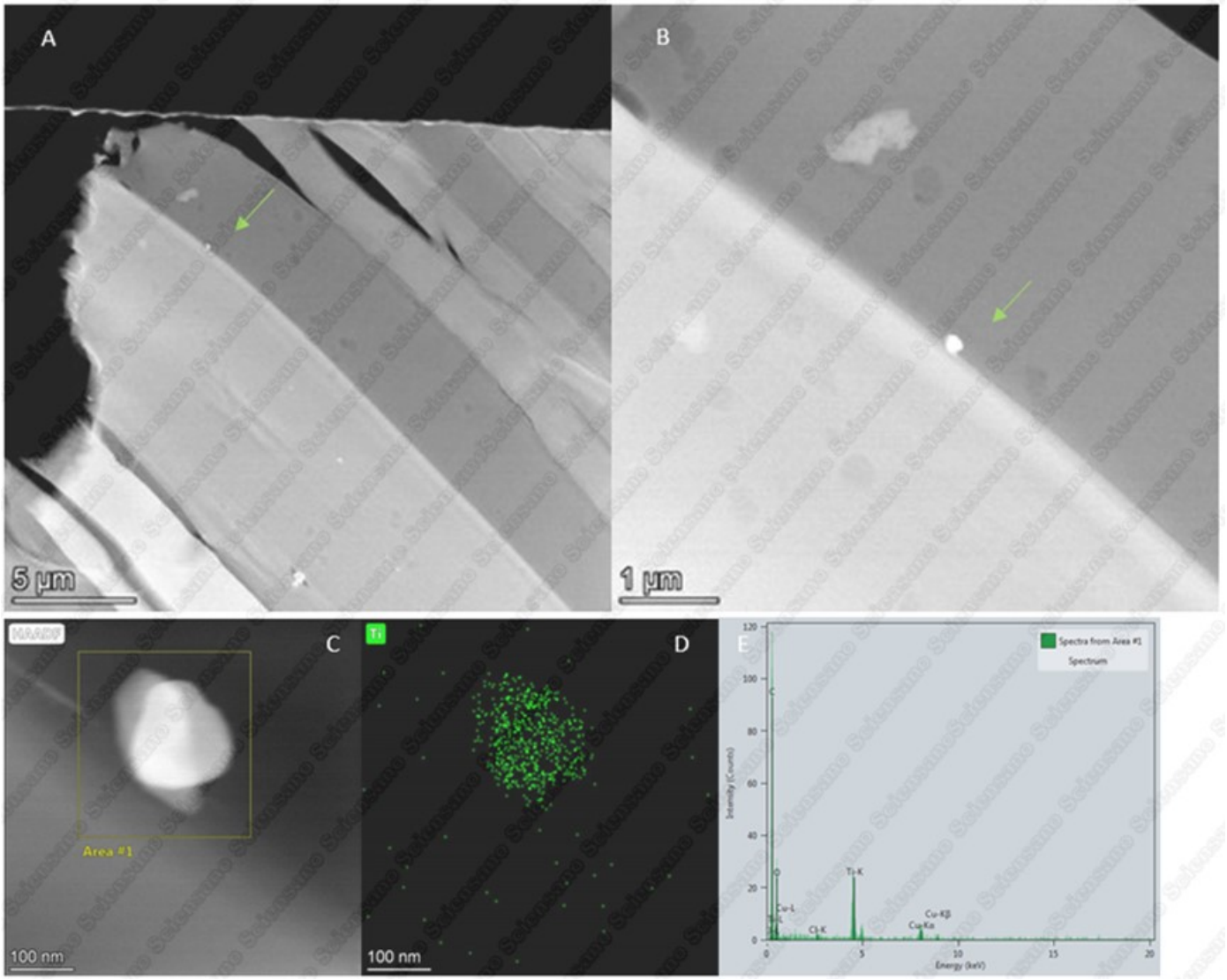

Figure 13 selected HAADF- STEM images at (A) low and (B) intermediate magnification, showing a particle at the edge of a polyester fiber (arrow) and corresponding EDX results with (C) the STEM image after analysis, (D) the spectral image of Ti, and (E) the spectrum of the region indicated in C.

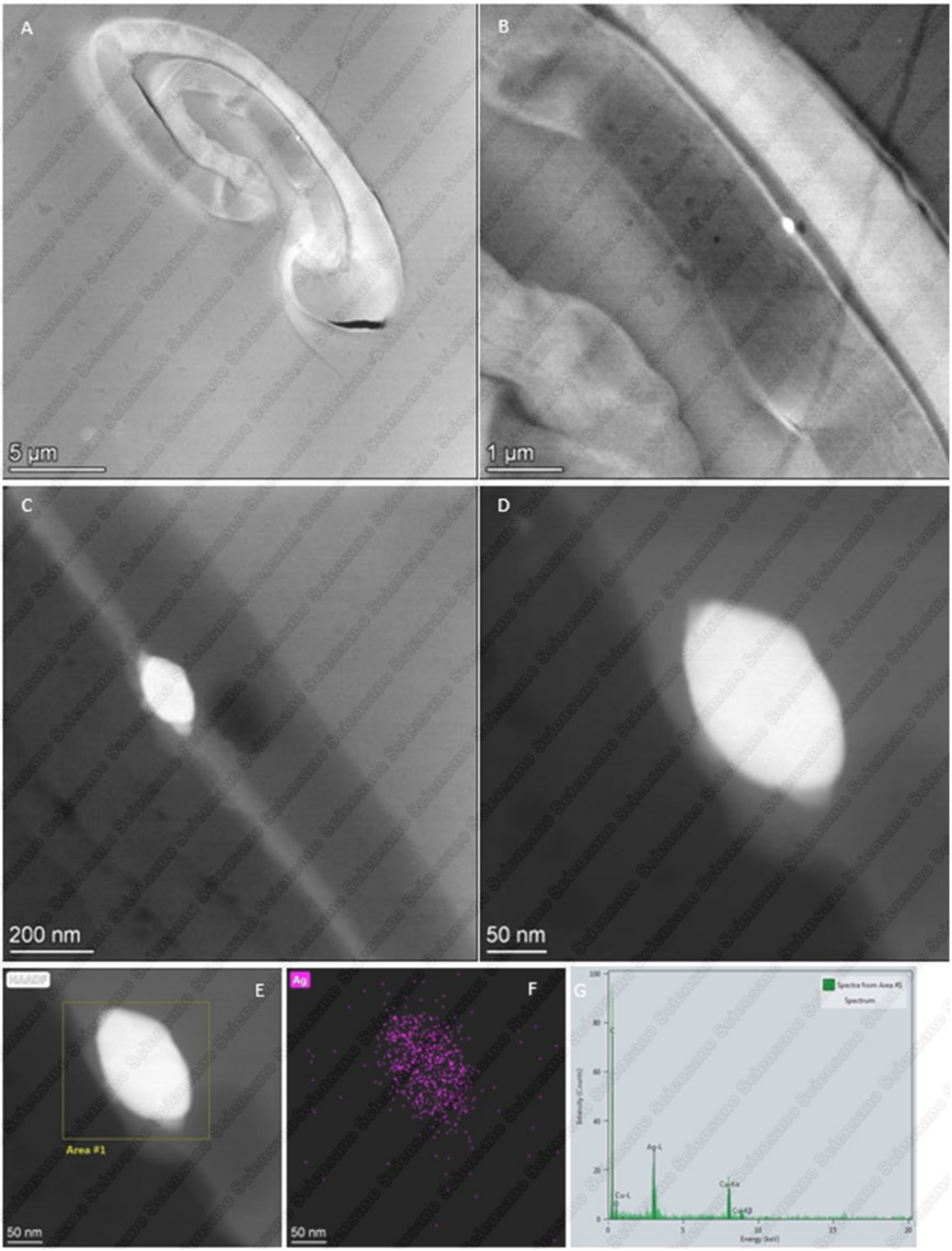

Figure 14 HAADF-STEM images at (A) low, (B) intermediate and (C,D) high magnification showing a particle on a coton fiber, and corresponding EDX results with (E) the STEM image after analysis, (F) the spectral image of Ag, and (G) the spectrum of the region indicated in E.

F.4 Sample T14G: External layer, repetition 2

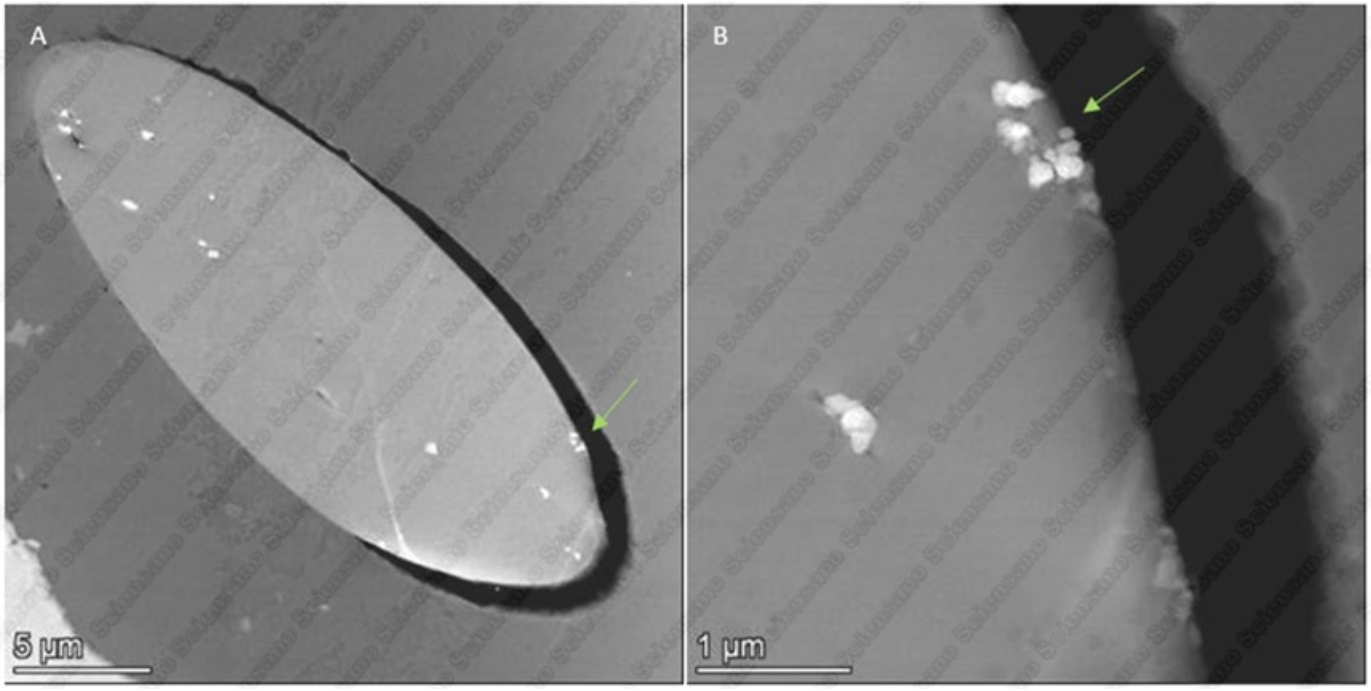

Figure 15 Representative HAADF-STEM images of sample T14G showing agglomerated near-spherical particles in cross sections of fibers at low (A) and high (B) magnifications. The agglomerate shown in figure B lies at the edge of the textile fiber shown in A (green arrow).

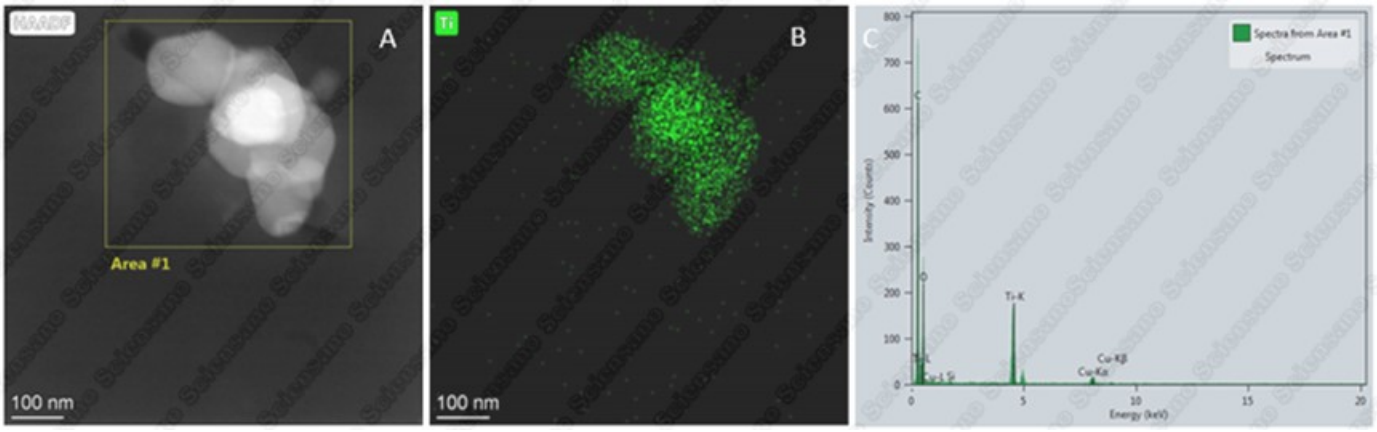

Figure 16 (A) HAADF-STEM image after analysis combined with (B) EDX spectral image of Ti and (C) EDX spectrum of the area indicated in A, demonstating that the particles found in the fibers of sample T14G are TiO_2 particles

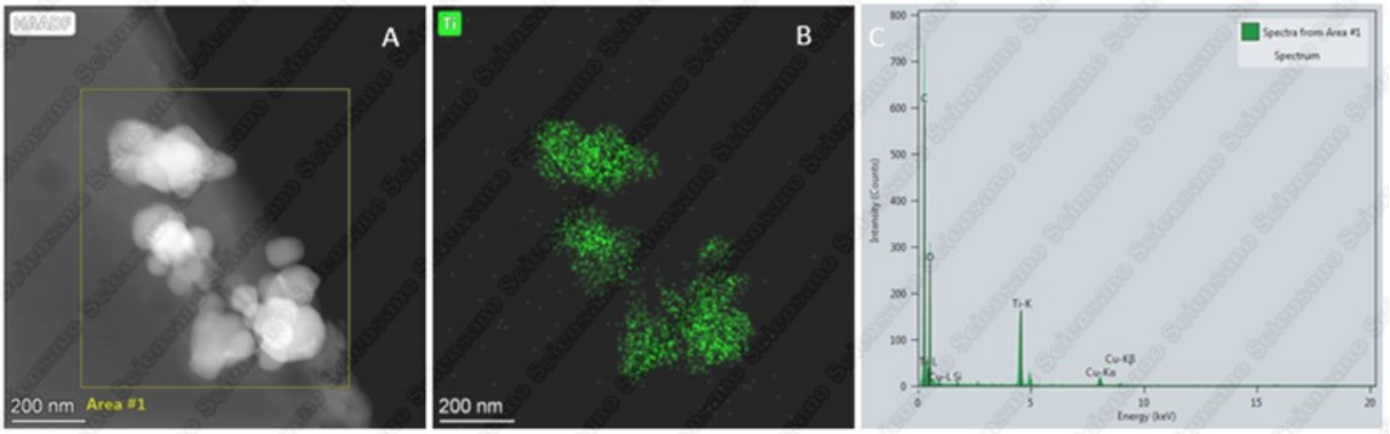

Figure 17 (A) HAADF-STEM image after analysis combined with (B) EDX spectral image of Ti and (C) EDX spectrum of the area indicated in A, demonstating that the agglomerate at the edge of a fiber shown in Figure 15 consists of TiO_2 particles.

F.5 Sample T14H: Middle layer, repetition 2

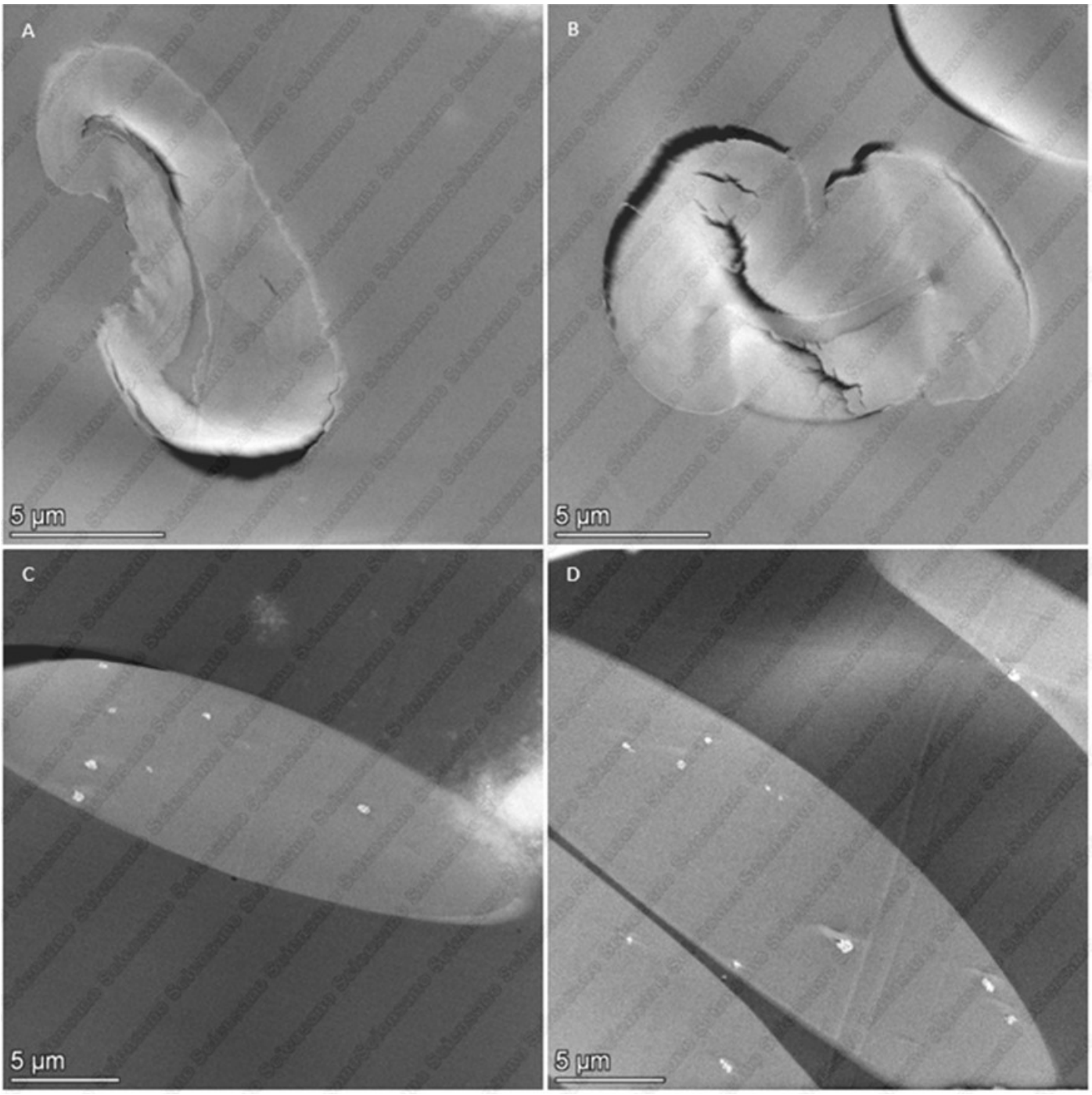

Figure 18 Representative STEM images of sample T14H showing two types of fibers present in the sample: (A, B) coton fibers showing a void or thinner region in the center, and (C, D) polyester fibers containing agglomerated near-spherical particles. Particles are generally located inside the fibers, although some particles are found at the edge of the fibers.

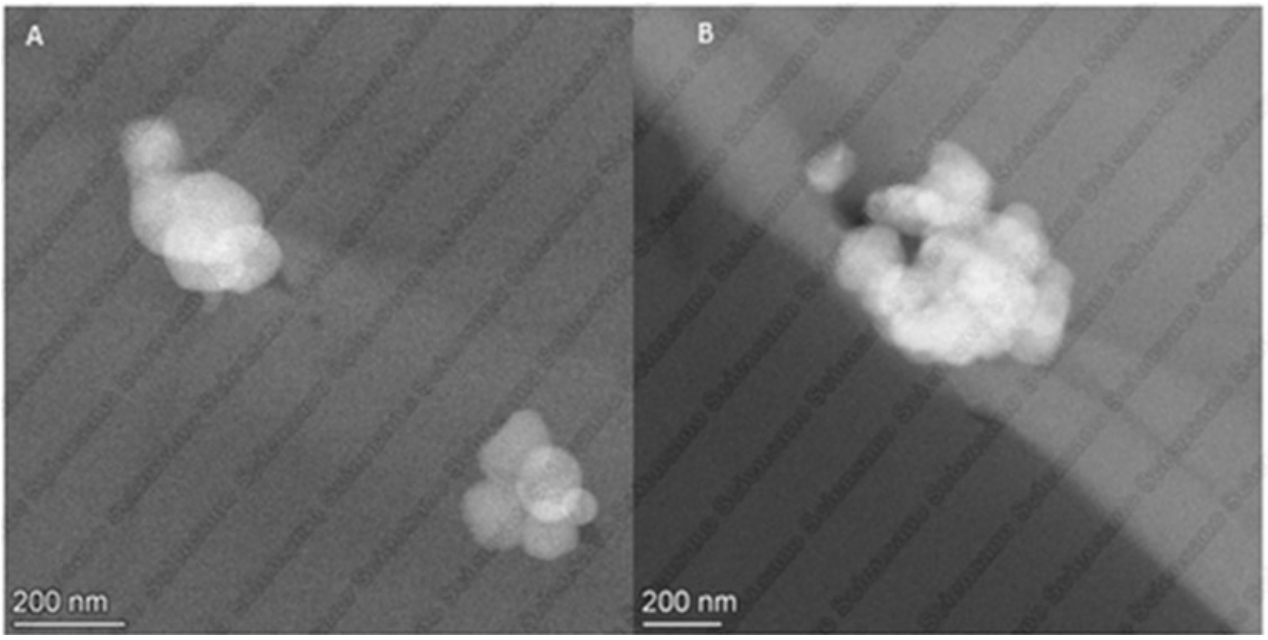

Figure 19 Selected HAADF-STEM images of sample T14H showing the agglomerated near-spherical particles in cross sections of polyester fibers at high magnifications. (A) Particles are generally located inside the fibers, although (B) some particles are found at the edge of the fibers.

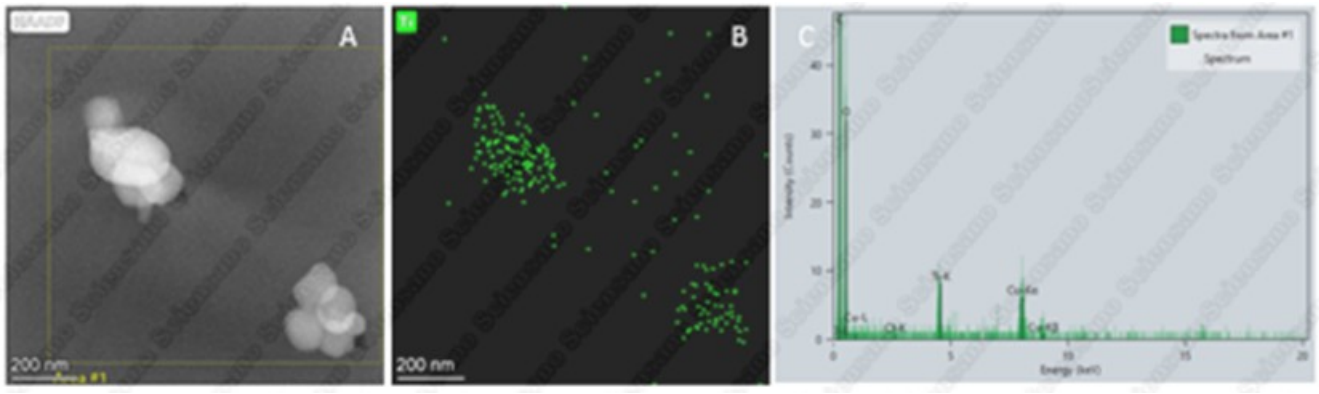

Figure 20 (A) HAADF-STEM image after analysis combined with (B) EDX spectral image of Ti and (C) EDX spectrum of the area indicated in A, demonstating that the particles found in the fibers of sample T14H are TiO_2 particles.

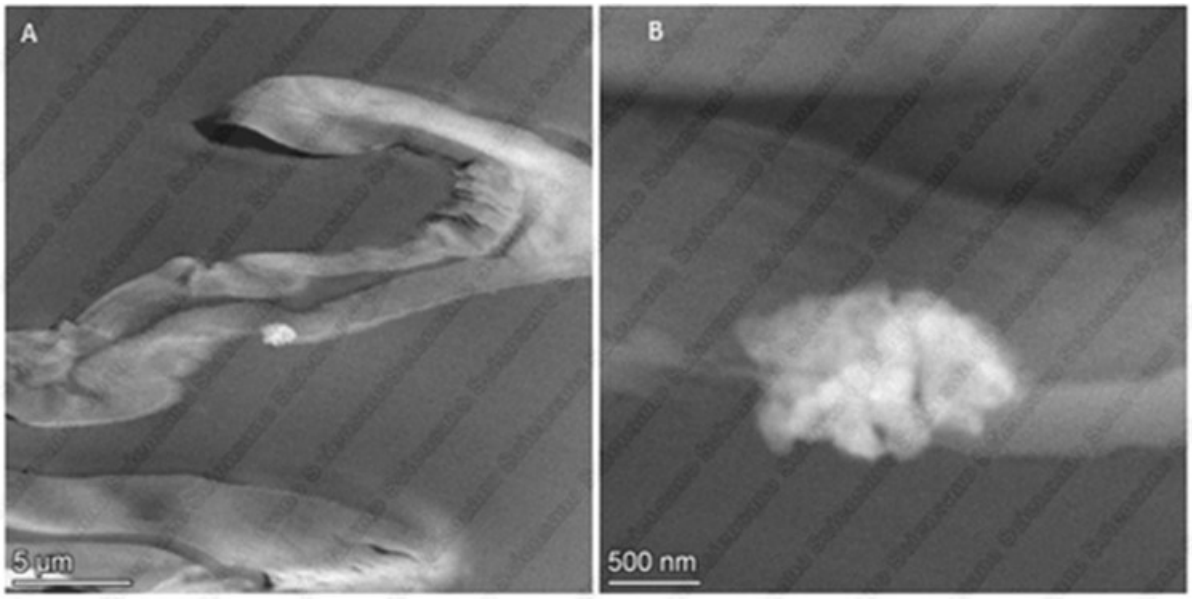

Figure 21 Selected HAADF-STEM images of sample T14H showing an agglomerate of TiO2 particles (confirmed by EDX, data not shown) at the edge of the coton fibers at (A) low and (B) high magnification.

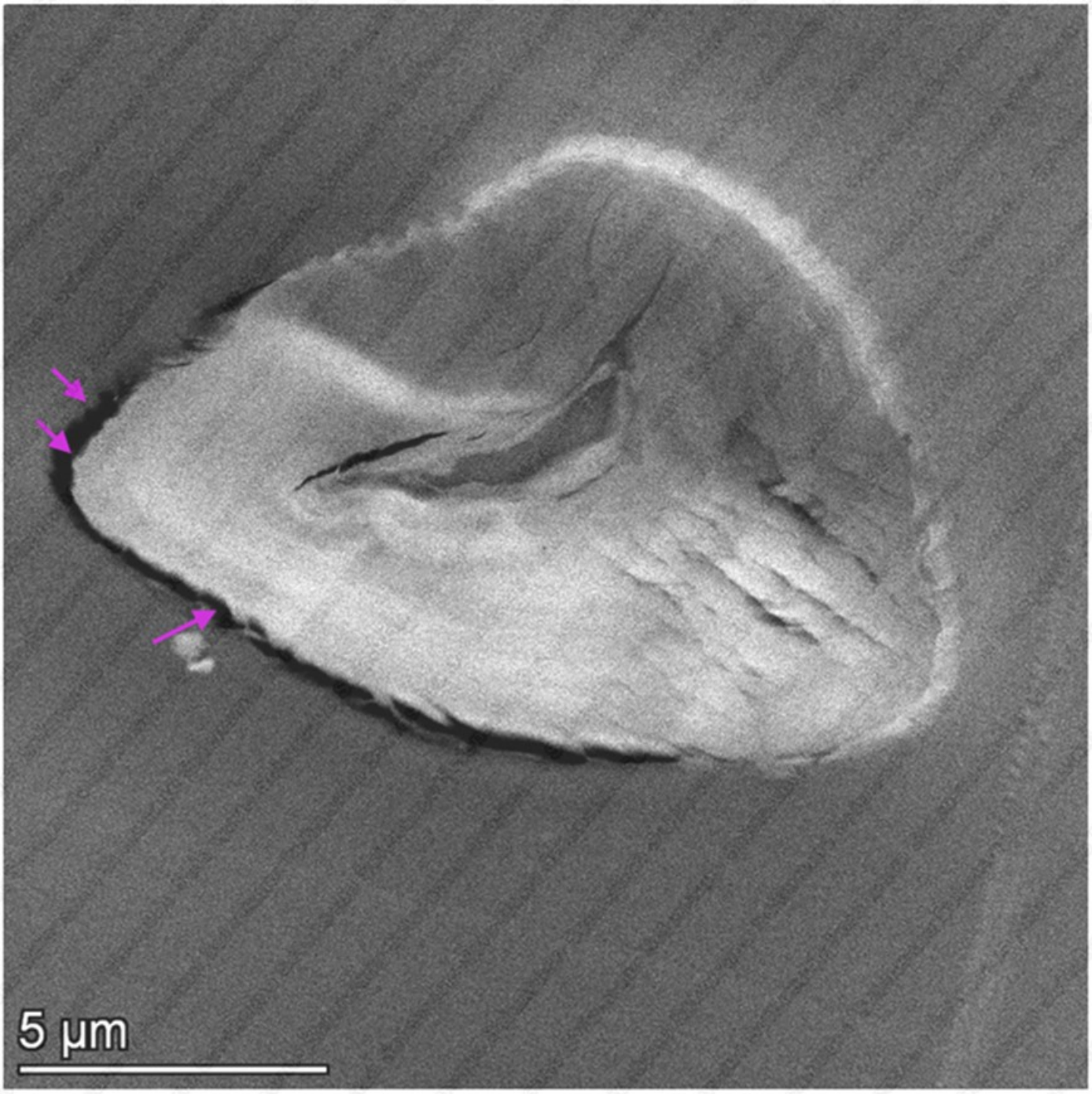

Figure 22 Selected HAADF-STEM image of a coton fiber where nanoparticles are observed at the edge of the fiber. The location of the particles is indicated by the pink arrows, but they are only visible at higher magnifications (see Figure 23, Figure 24 and Figure 25).

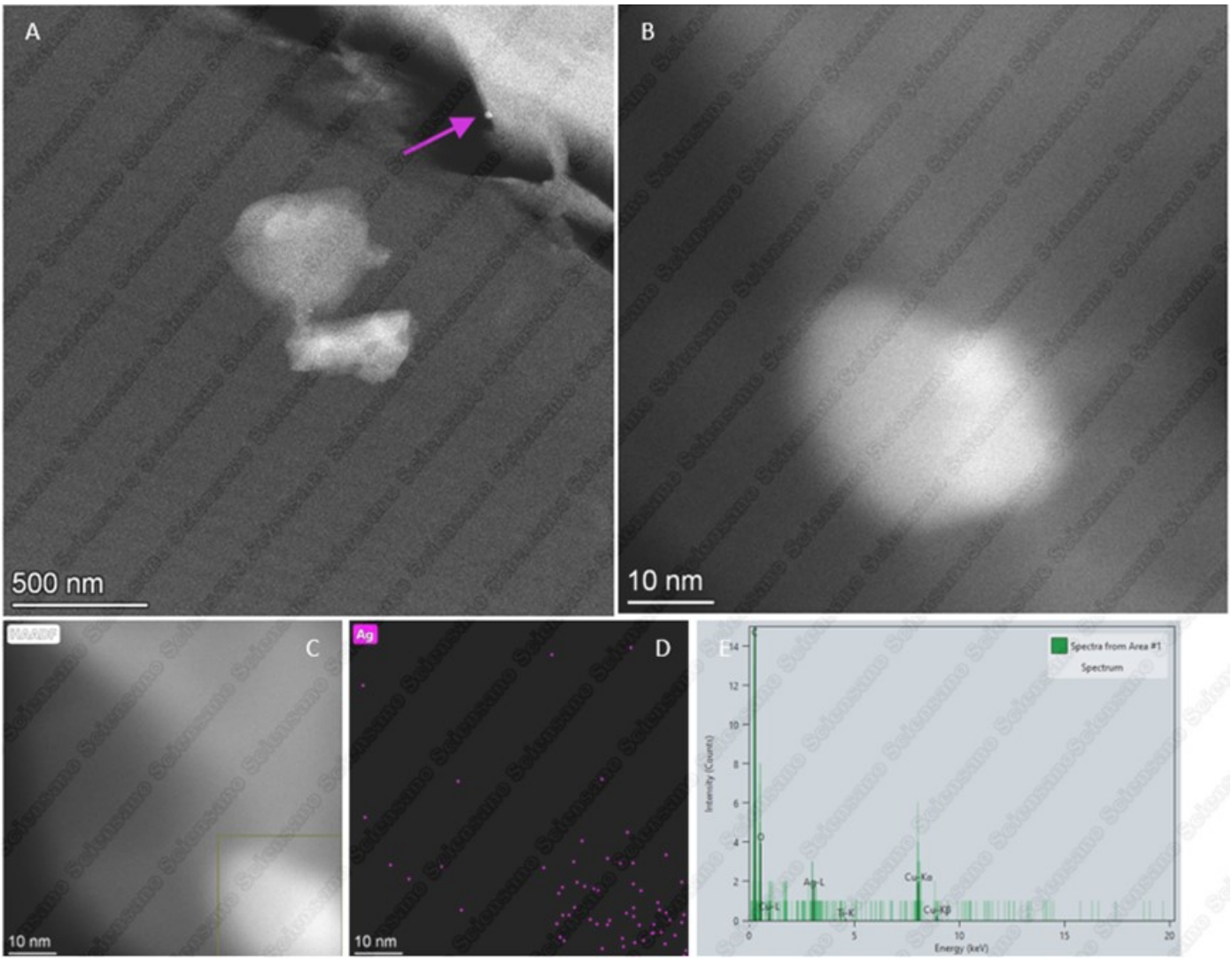

Figure 23 Selected HAADF-STEM images at (A) intermediate and (B) high magnifications of a region indicated in Figure 22 containing a nanoparticle (pink arrow), and corresponding EDX results with (C) the STEM image after analysis, (D) the spectral image of Ag and (E) the spectrum of the region indicated in C.

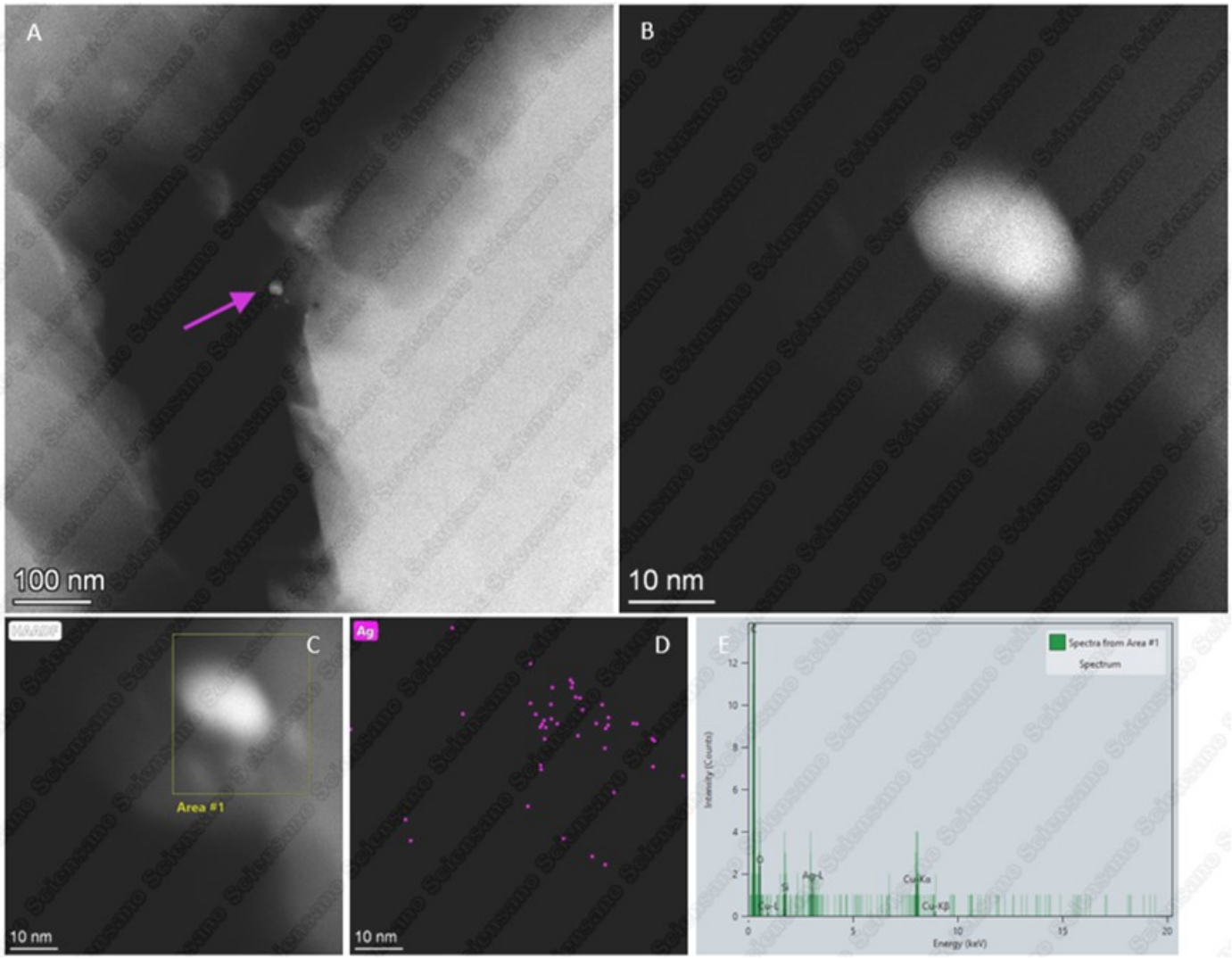

Figure 24 Selected HAADF-STEM images at (A) intermediate and (B) high magnifications of a region indicated in Figure 22 containing a nanoparticle (pink arrow), and corresponding EDX results with (C) the STEM image after analysis, (D) the spectral image of Ag and (E) the spectrum of the region indicated in C.

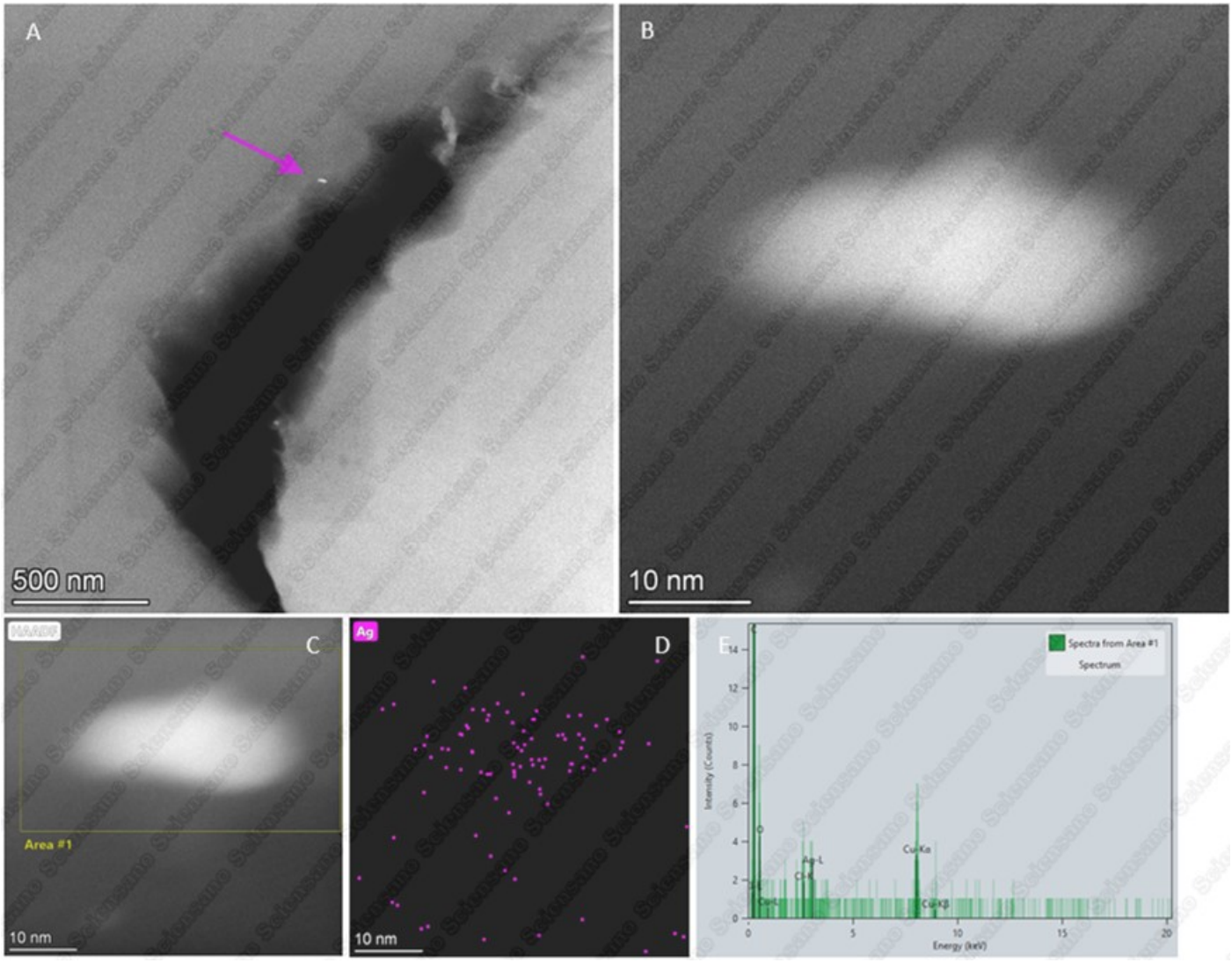

Figure 25 Selected HAADF-STEM images at (A) intermediate and (B) high magnifications of a region indicated in Figure 22 containing a nanoparticle (pink arrow), and corresponding EDX results with (C) the STEM image after analysis, (D) the spectral image of Ag and (E) the spectrum of the region indicated in C.

F.6 Sample T14I: Internal layer, repetition 2

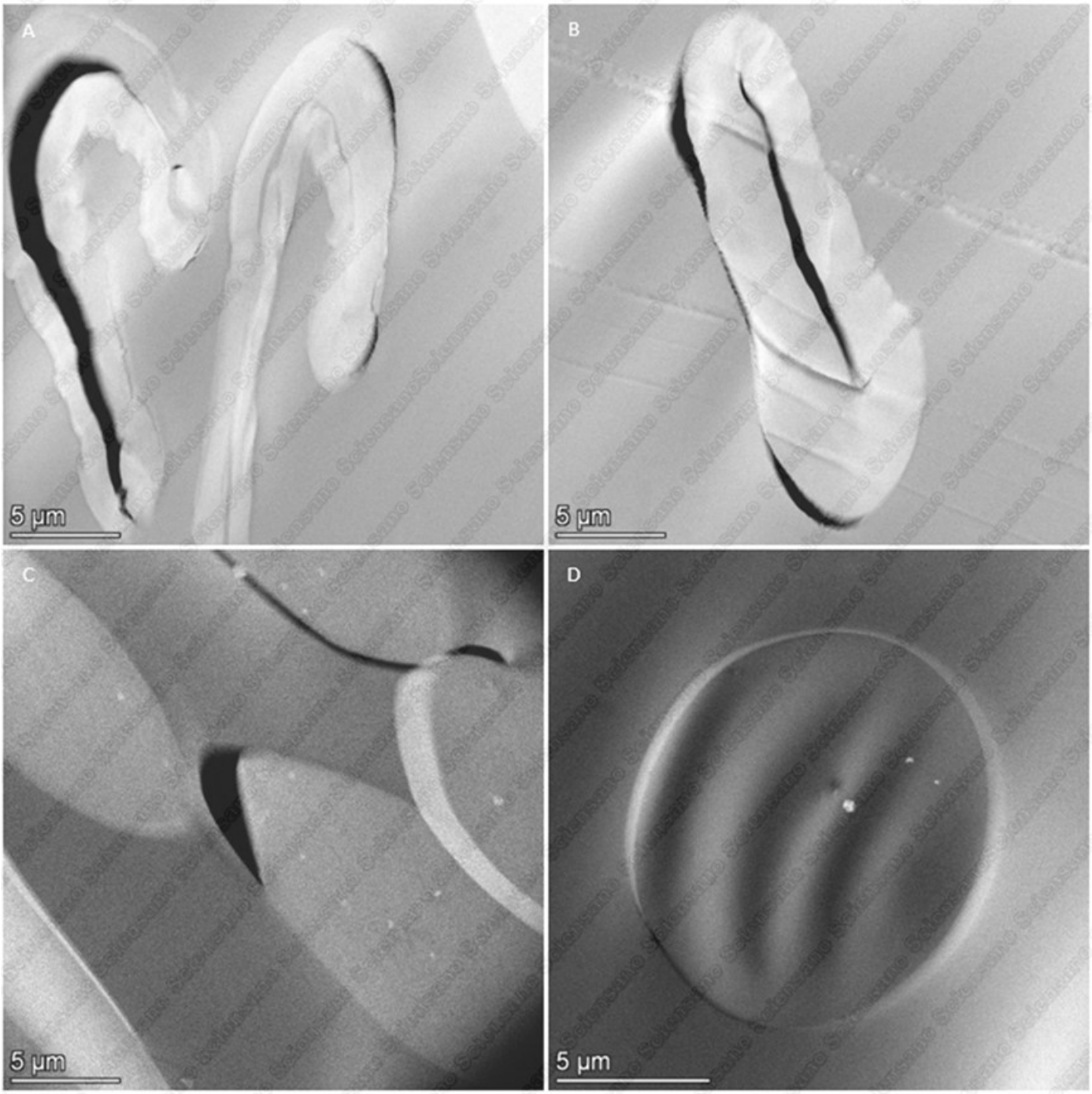

Figure 26 Representative HAADF-STEM images of sample T14I showing two types of fibers present in the sample: (A, B) coton fibers showing a void or thinner region in the center and (C, D) polyester fibers containing agglomerated near-spherical particles (C, D). Particles are generally located inside the fibers, although some particles are found at the edge of the fibers.

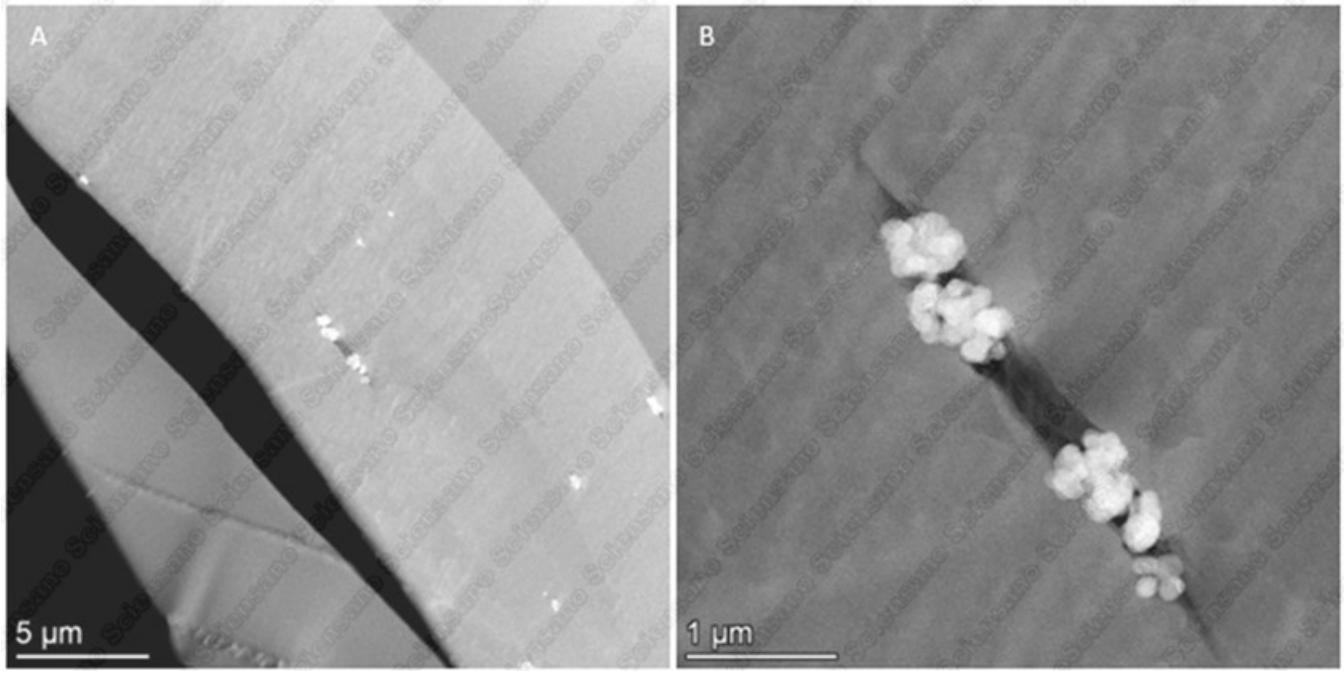

Figure 27 Representative HAADF-STEM images of sample T14I showing the agglomerated near-spherical particles in cross sections of fibers at (A) intermediate and (B) high magnifications.

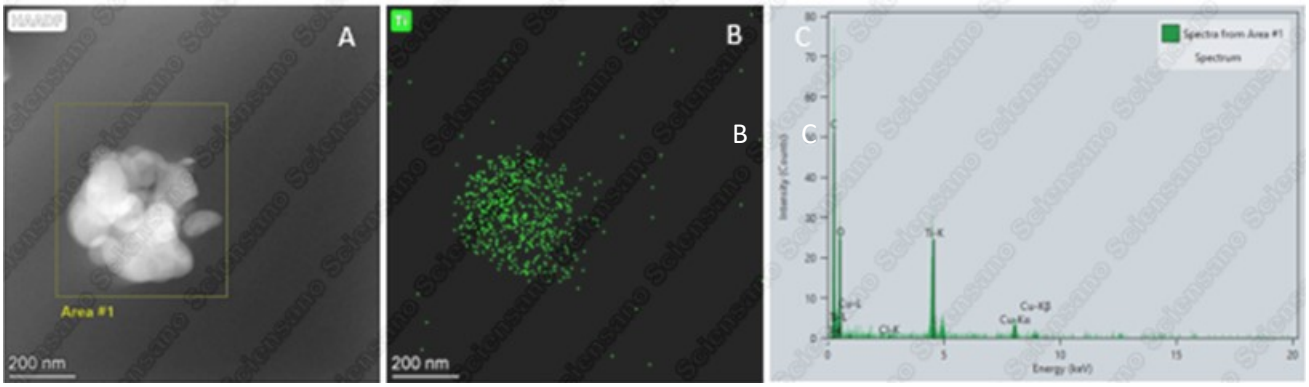

Figure 28 (A) HAADF-STEM image after analysis of an agglomerate of near-spherical particles at the center of a polyester fiber, combined with (B) EDX spectral image of Ti and (C) EDX spectrum of the area indicated in A, demonstating that the particles found in the polyester fibers of sample T14I are TiO_2 particles.

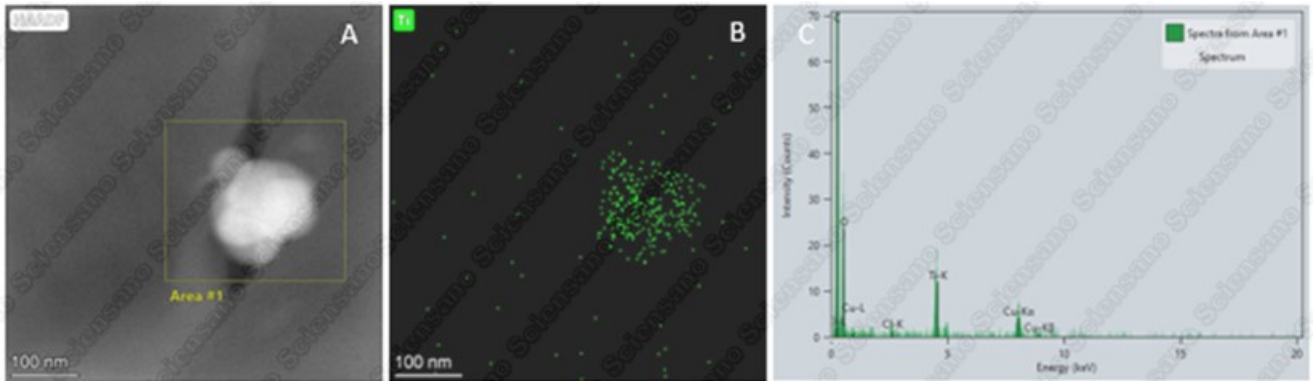

Figure 29 (A) HAADF-STEM image after analysis of an agglomerate of near-spherical particles at the edge of a polyester fiber, combined with (B) EDX spectral image of Ti and (C) EDX spectrum of the area indicated in A, demonstating that the particles are TiO_2 particles.

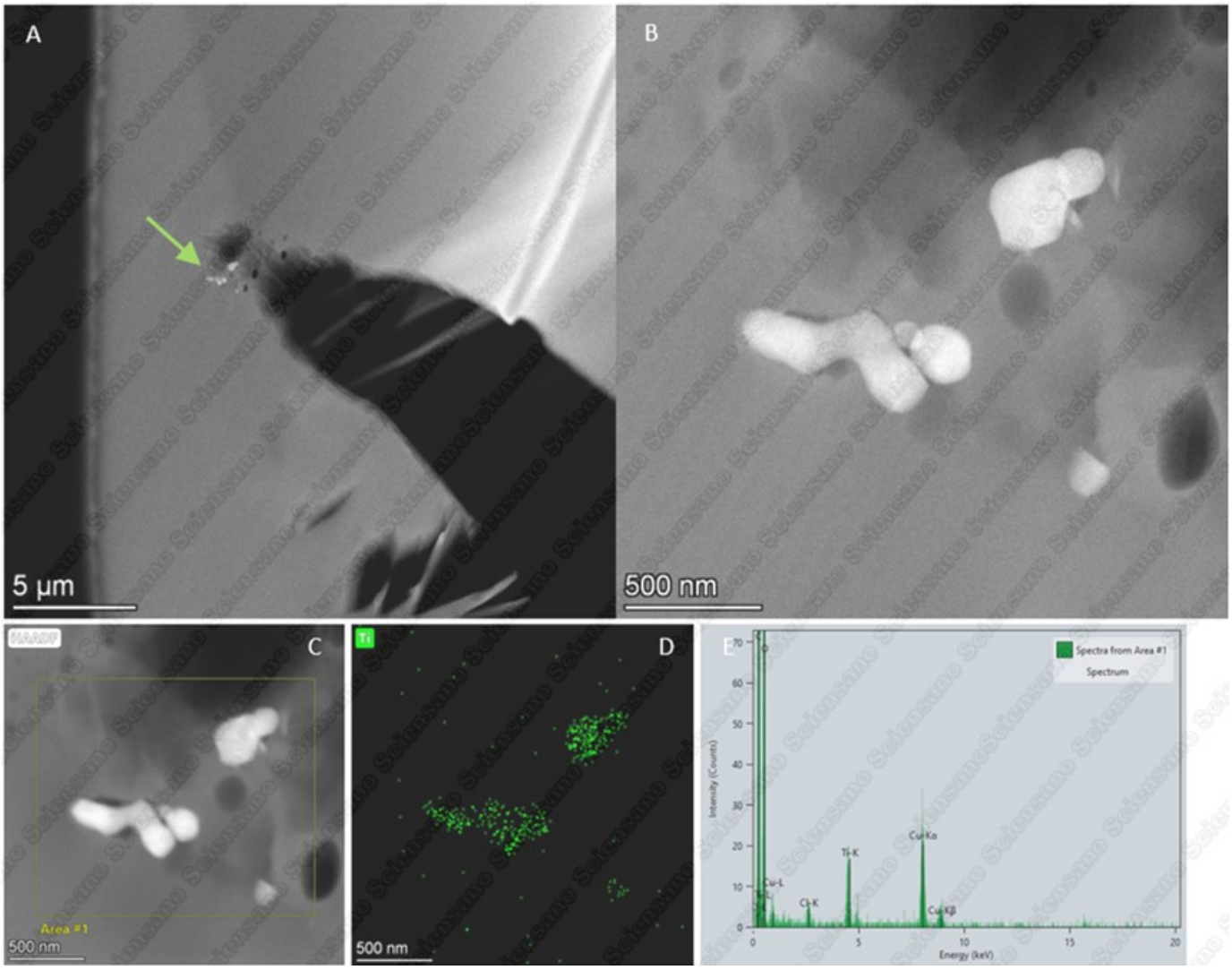

Figure 30 Selected HAADF-STEM images at (A) low and (B) high magnifications showing near-spherical agglomerated particles outside of the fibers, and corresponding EDX results showing that these are TiO2 particles, with (C) the STEM image after analysis, (D) the Ti spectral image and (E) the spectrum of the region indicated in C.

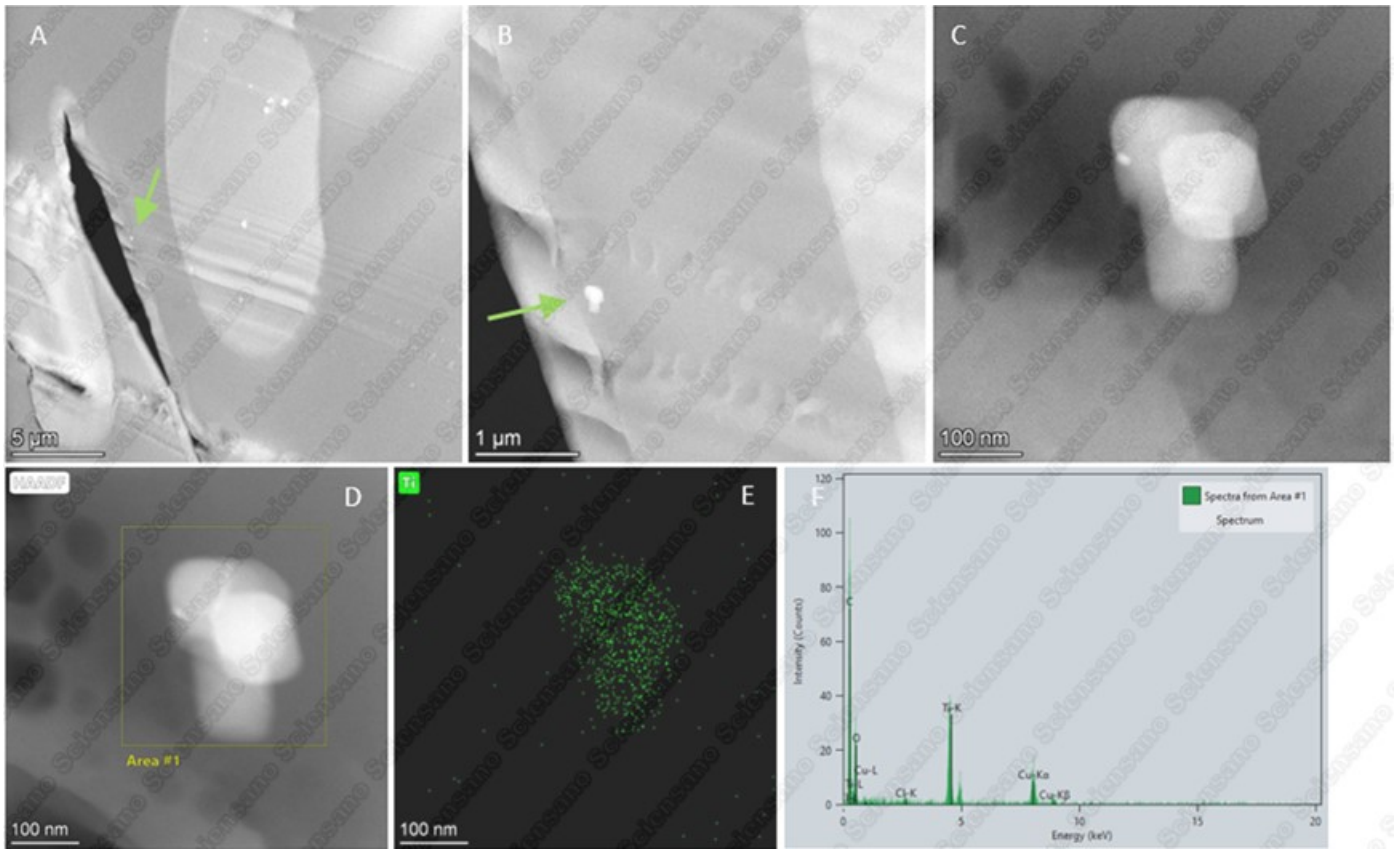

Figure 31 Selected HAADF-STEM images at (A) low (green arrow), (B) intermediate (green arrow) and (C) high magnifications showing near-spherical agglomerated particles outside of the fibers, and corresponding EDX results showing that these are TiO_2 particles, with (D) the STEM image after analysis, (E) the Ti spectral image and (F) the spectrum of the region indicated in D.

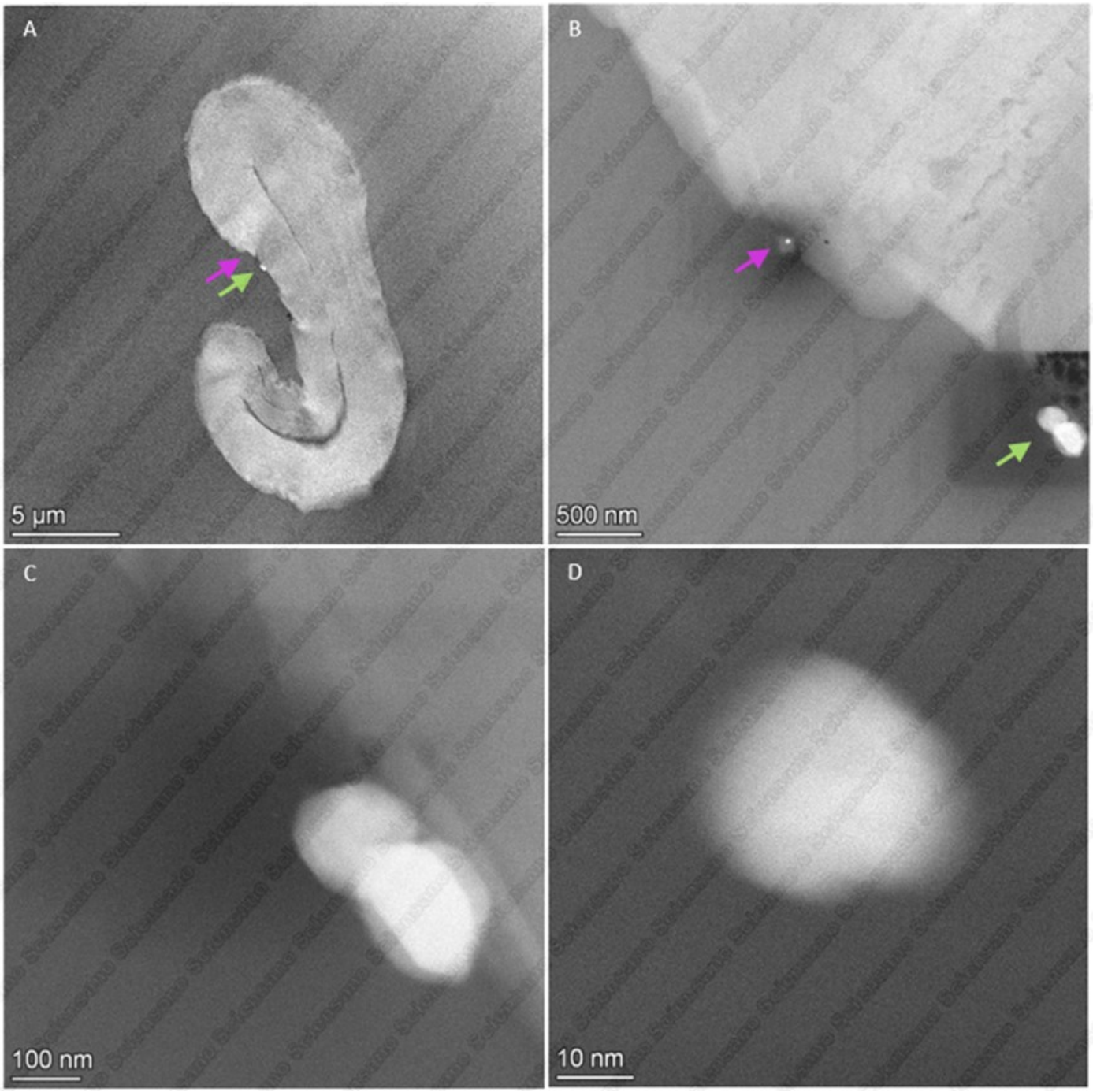

Figure 32 Selected HAADF-STEM images of a coton fiber showing two types of particles at the edge at (A) low (green and pink arrows) (B) intermediate (green and pink arrows) and (C, D) high magnifications.

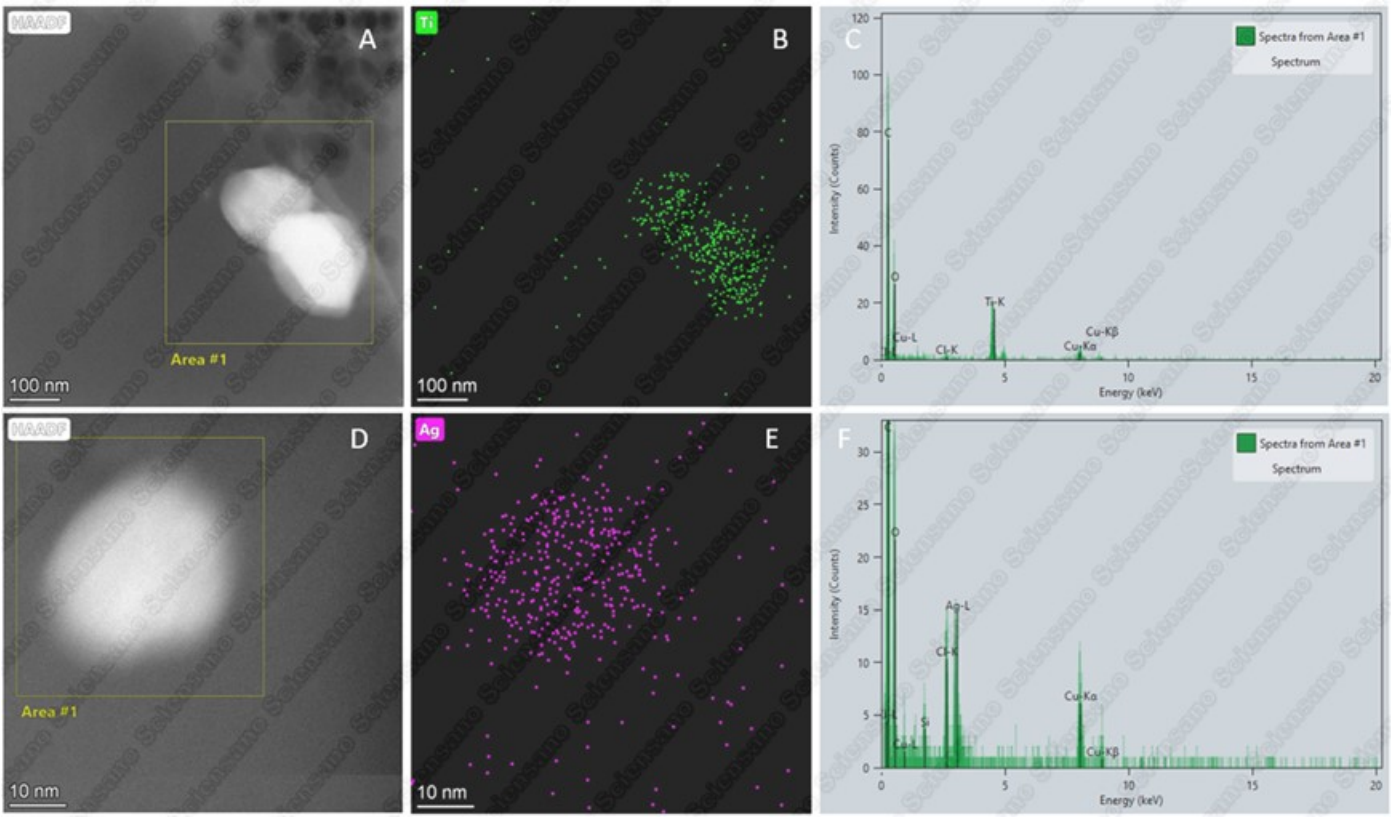

Figure 33 EDX results corresponding with the particles shown in Figure 32 showing that these are TiO_2 and Ag particles, with (A, D) the STEM images after analysis, (B, E) the Ti and Ag spectral images and (C, F) the spectra of the regions indicated in A and D.

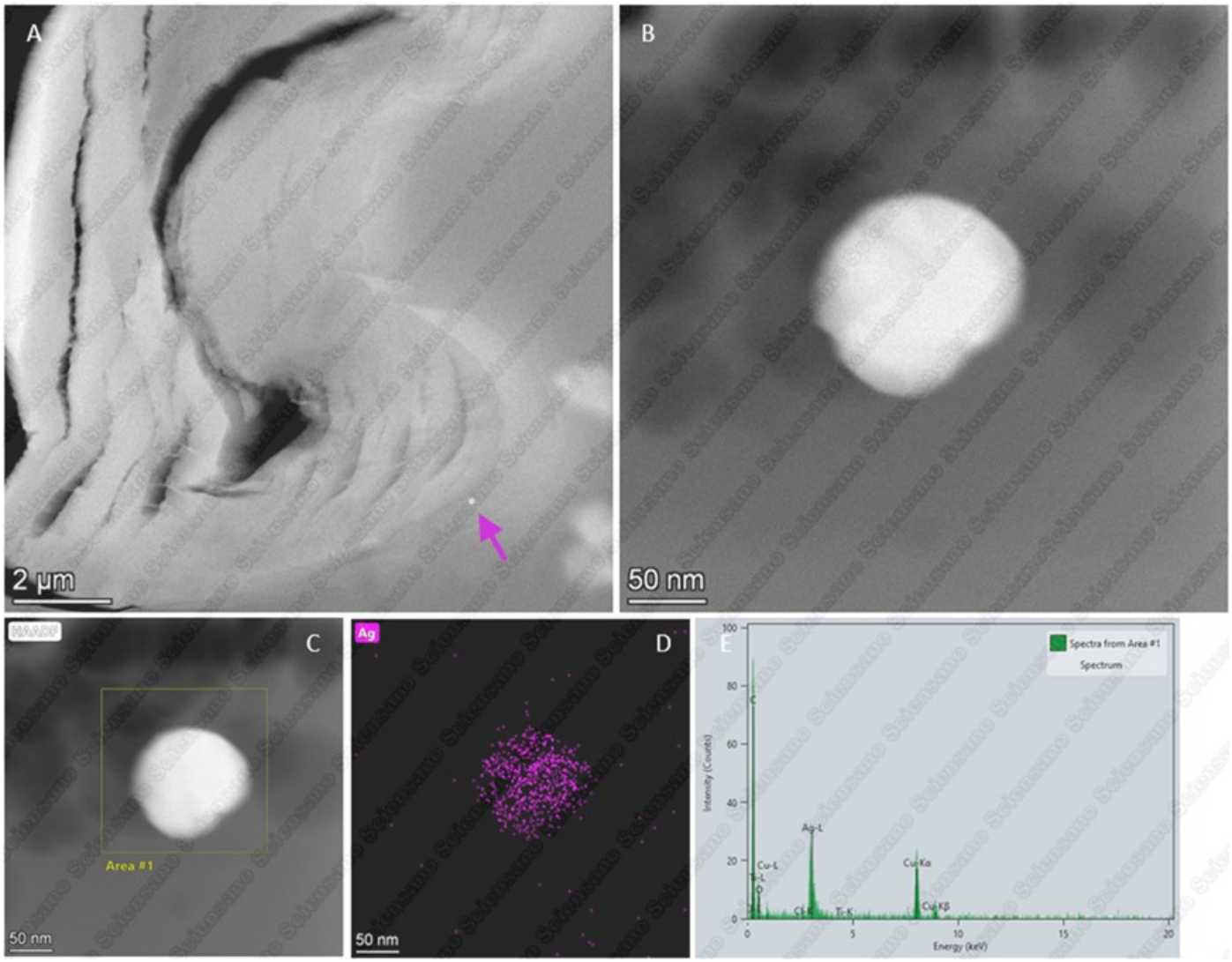

Figure 34 Selected HAADF-STEM images at (A) low and (B) high magnifications of the edge of a coton fiber containing a nanoparticle (pink arrow), and corresponding EDX results with (C) the STEM image after analysis, (D) the spectral image of Ag and (E) the spectrum of the region indicated in C.

F.7 Sample T17A: External layer, repetition 3

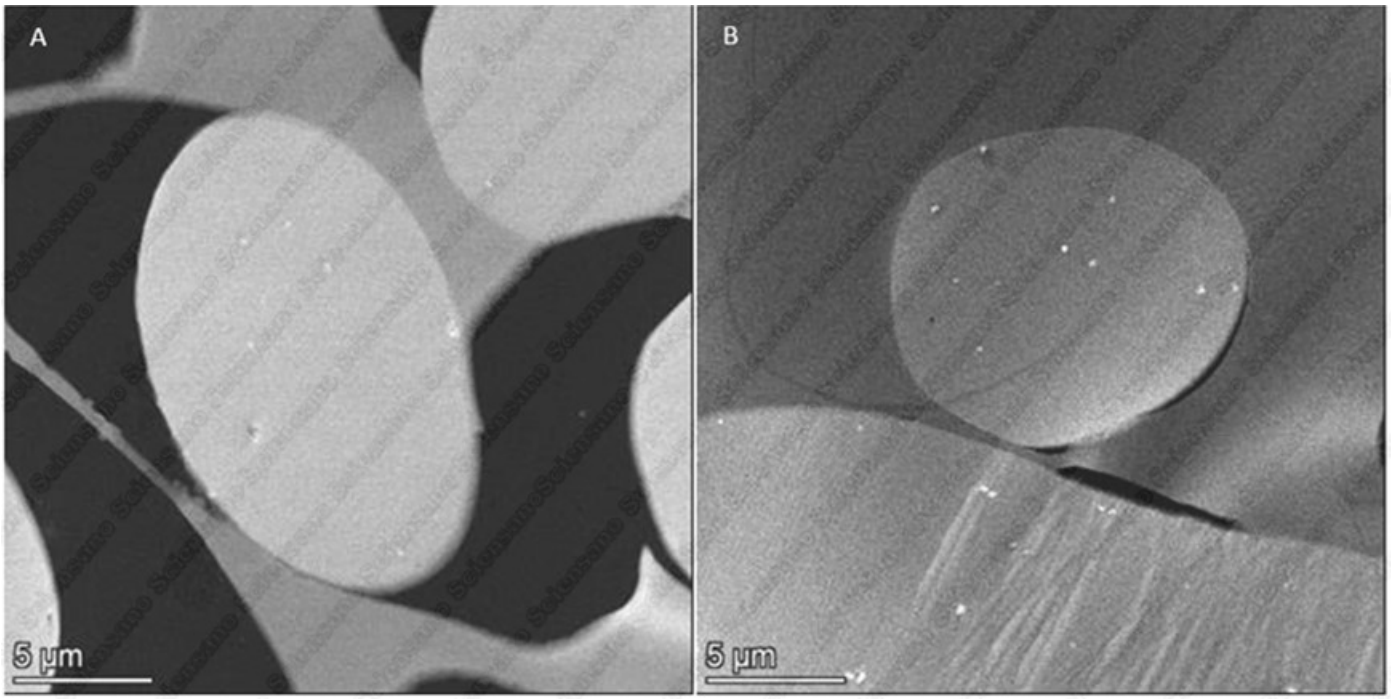

Figure 35 Representative HAADF-STEM images of sample T17A showing agglomerated near-spherical particles in cross sections of fibers.

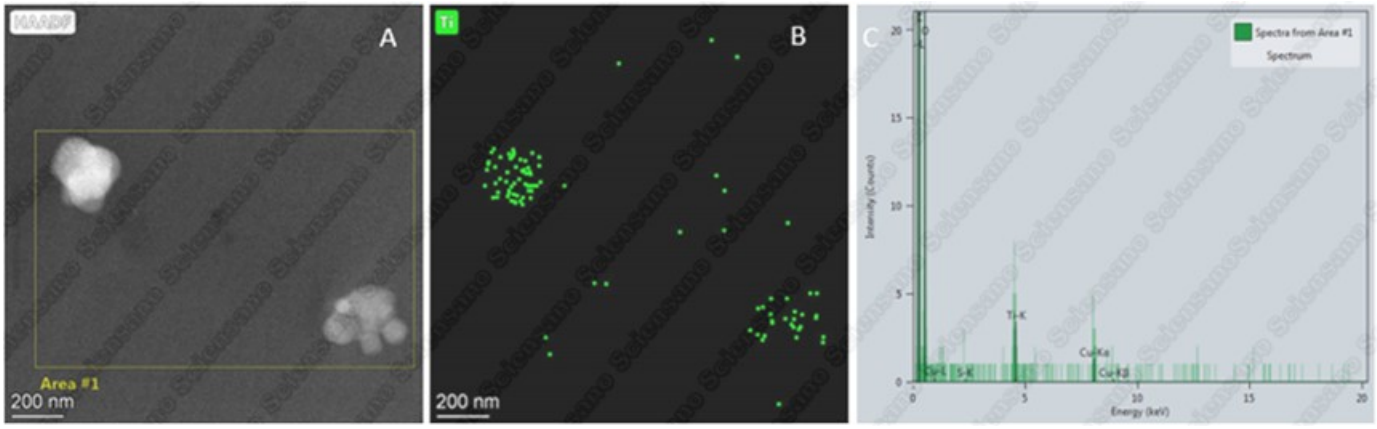

Figure 36 (A) HAADF-STEM image after analysis combined with (B) EDX spectral image of Ti and (C) EDX spectrum of the area indicated in A, demonstating that the particles found in the fibers of sample T17A are TiO_2 particles.

F.8 Sample T17B: Middle layer, repetition 3

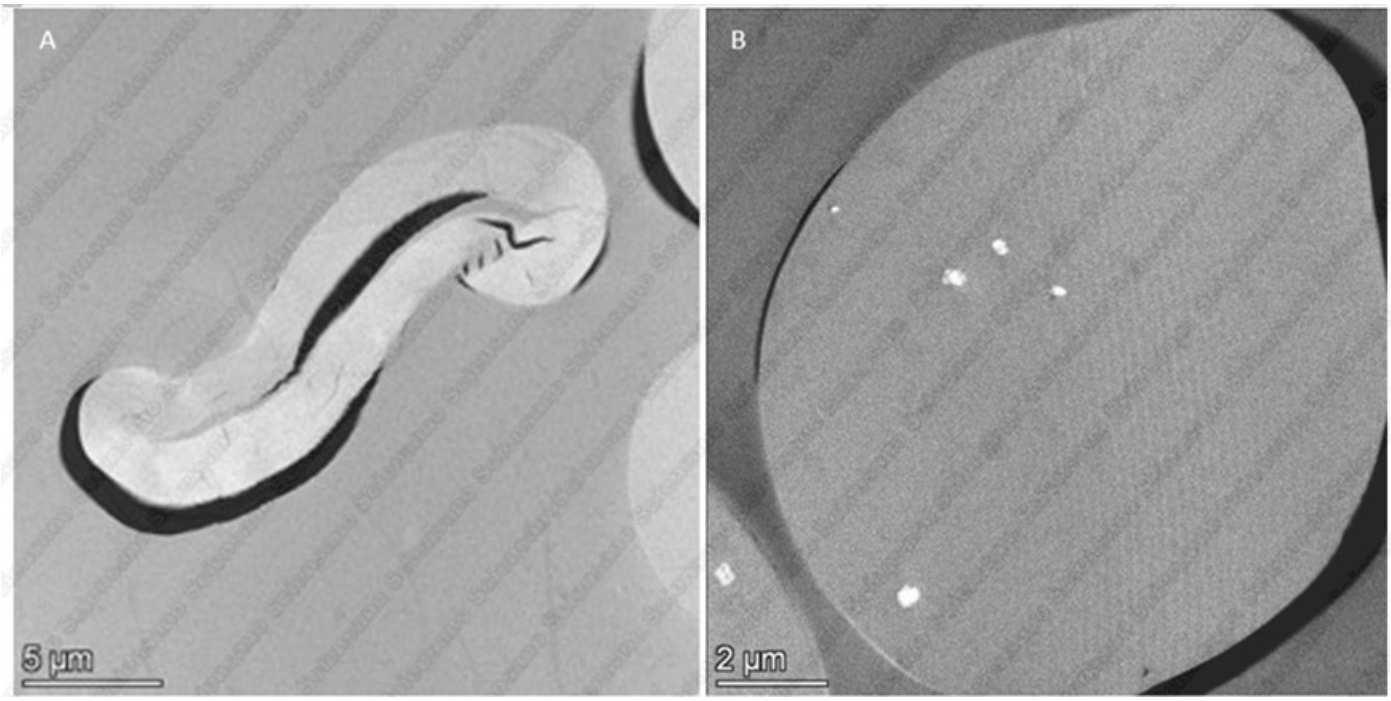

Figure 37 Representative HAADF-STEM images of sample T17B, showing two types of fibers present in the sample: (A) a coton fiber showing a void or thinner region in the center and (B) a polyester fiber containing agglomerated near-spherical particles.

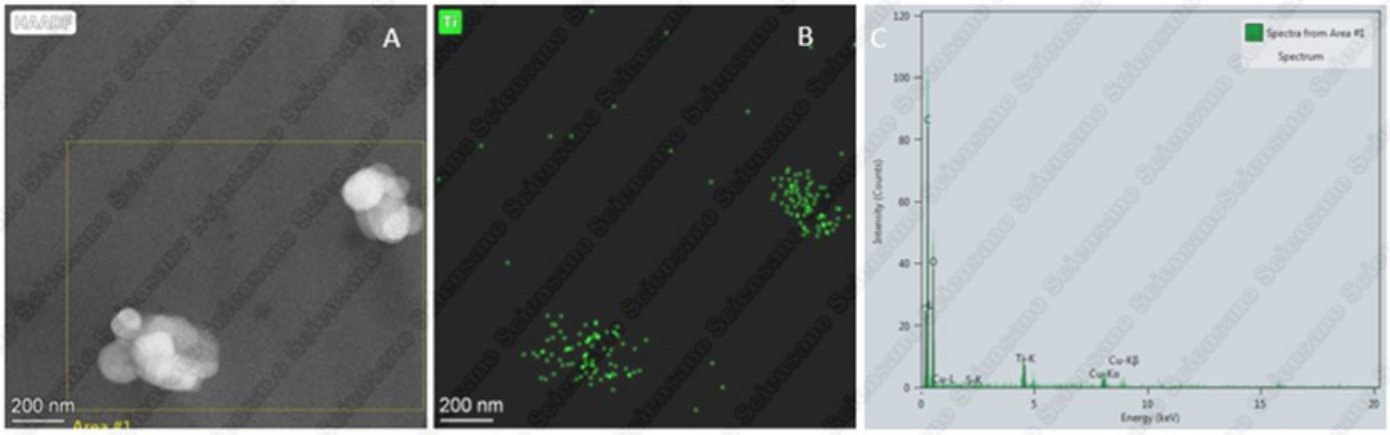

Figure 38 (A) HAADF-STEM image after analysis combined with (B) EDX spectral image of Ti and (C) EDX spectrum of the area indicated in A, demonstating that the particles found in the polyester fibers of sample T17B are TiO_2 particles.

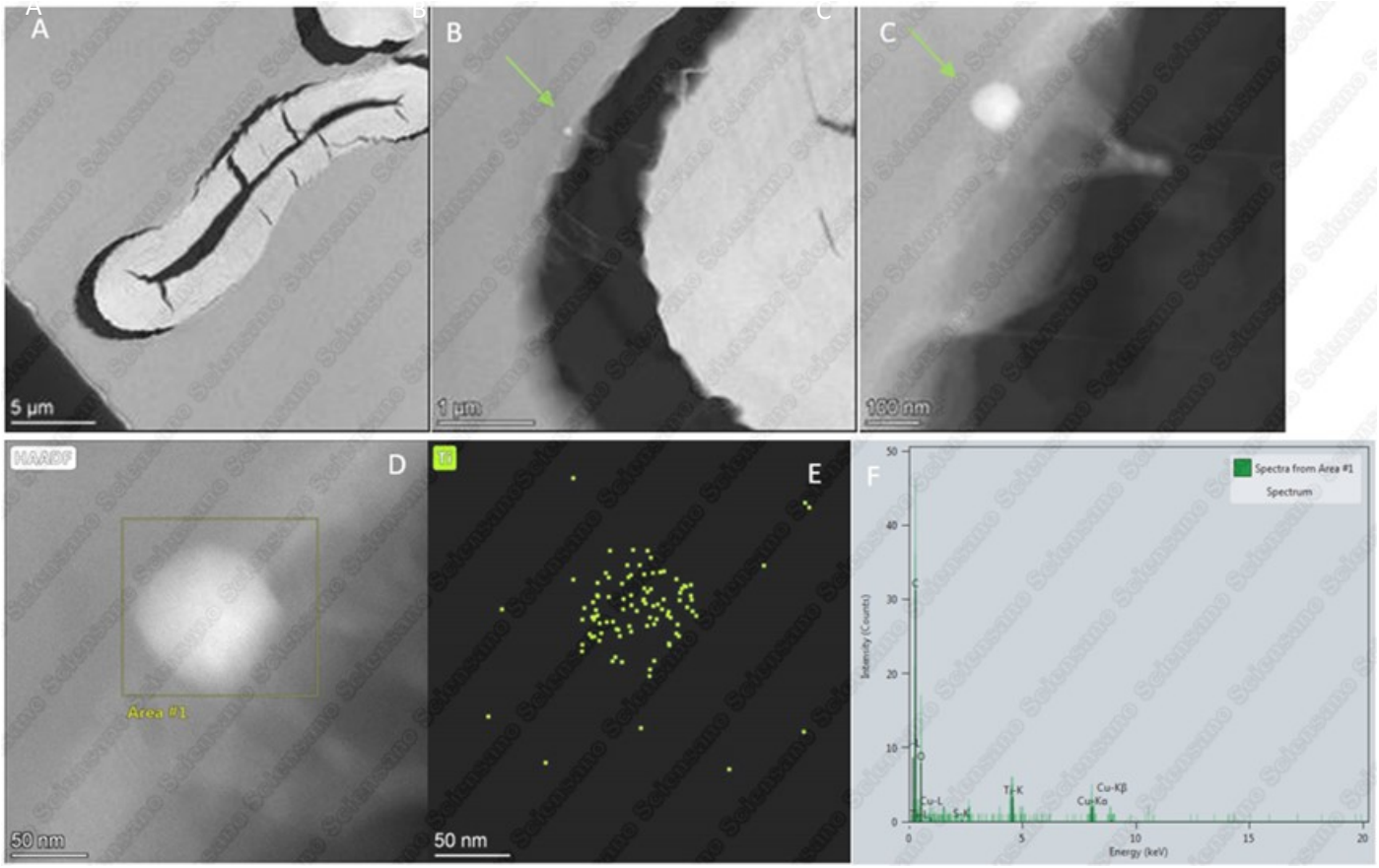

Figure 39 Selected HAADF-STEM images at (A) low, (B) intermediate and (C) high magnifications of the edge of a coton fiber containing a nanoparticle (green arrow), and corresponding EDX results with (D) the STEM image after analysis, (E) the spectral image of Ti and (F) the spectrum of the region indicated in D.

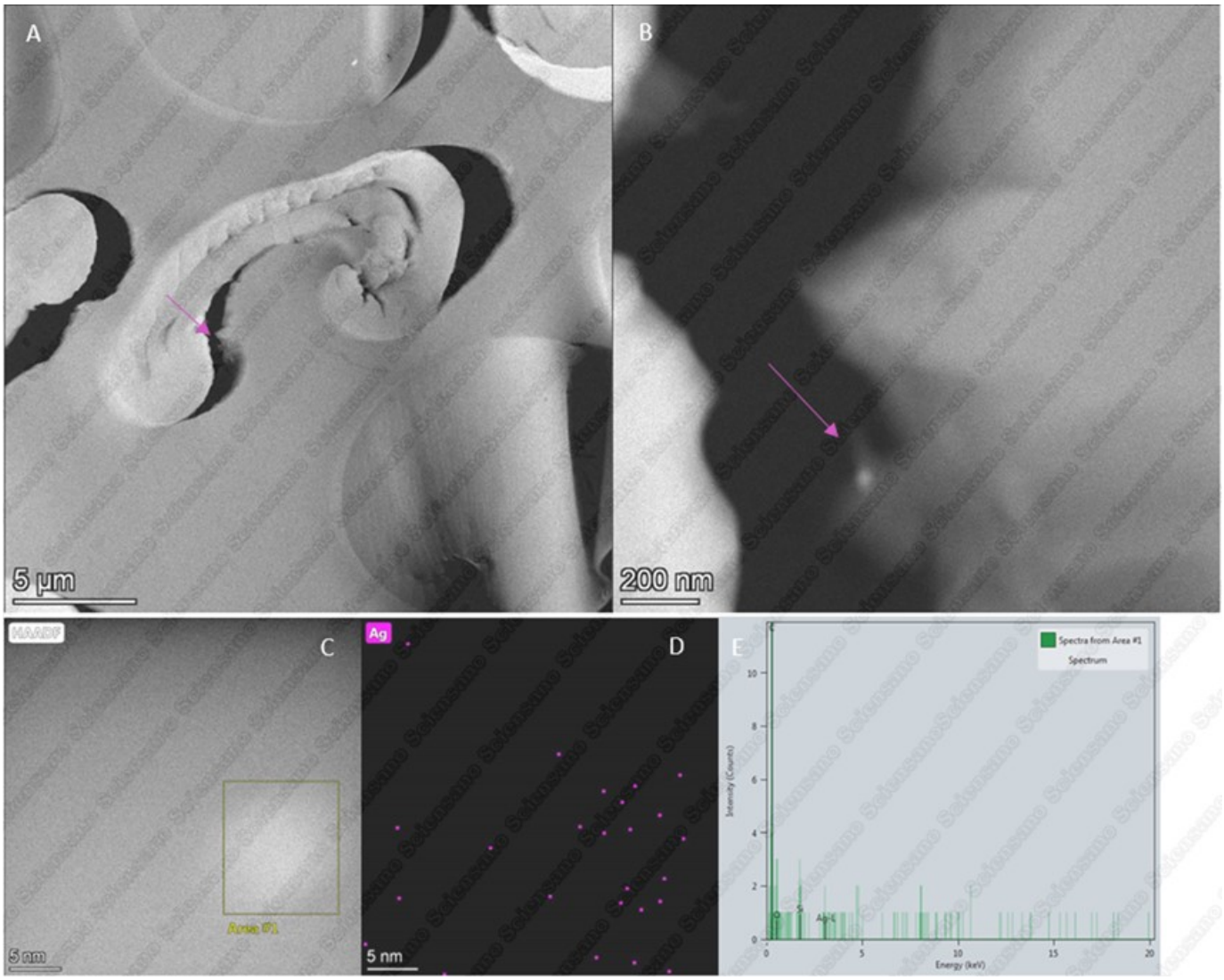

Figure 40 Selected HAADF-STEM images at (A) low and (B) high magnifications of the edge of a coton fiber containing a nanoparticle (pink arrow), and corresponding EDX results with (C) the STEM image after analysis, (D) the spectral image of Ag and (E) the spectrum of the region indicated in C. Only a very weak Ag signal was measured.

F.9 Sample T17C: Internal layer, repetition 3

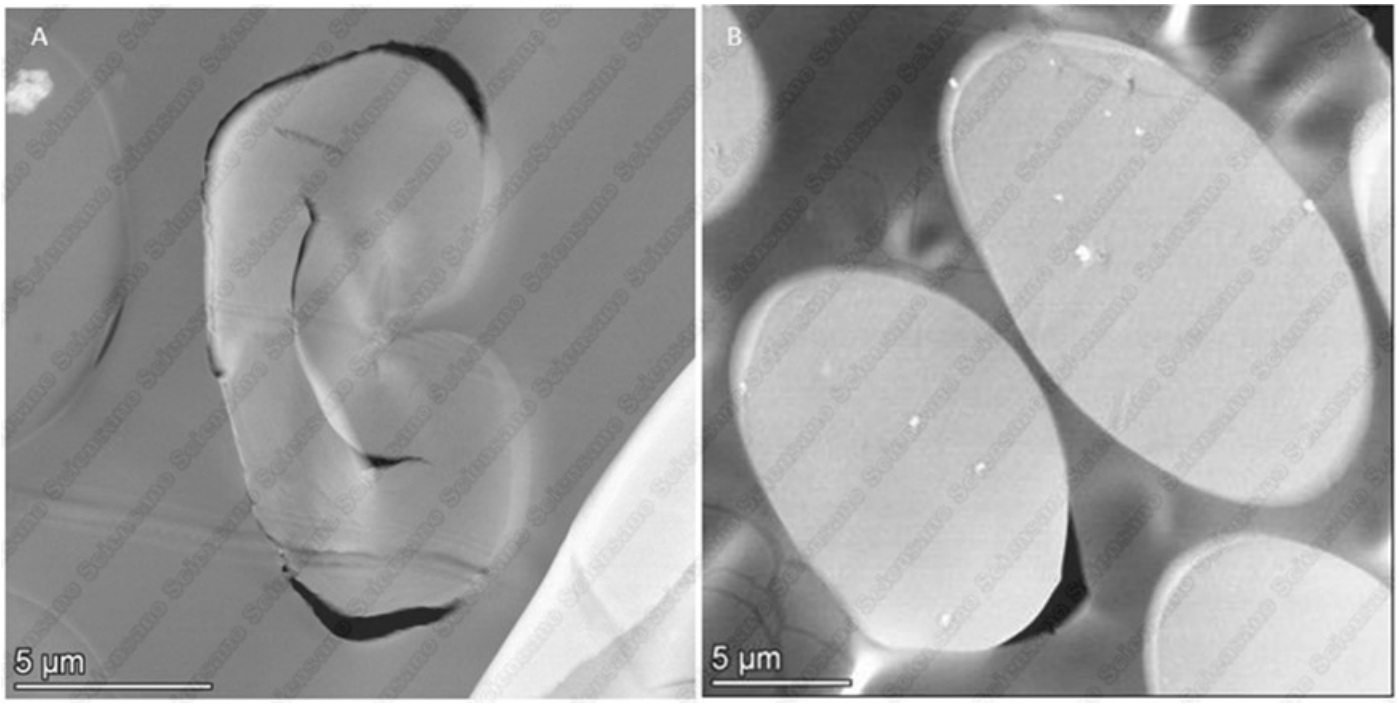

Figure 41 Representative HAADF-STEM images of sample T17C, showing two types of fibers present in the sample: (A) a coton fiber showing a void or thinner region in the center and (B) a a polyester fiber containing agglomerated near-spherical particles.

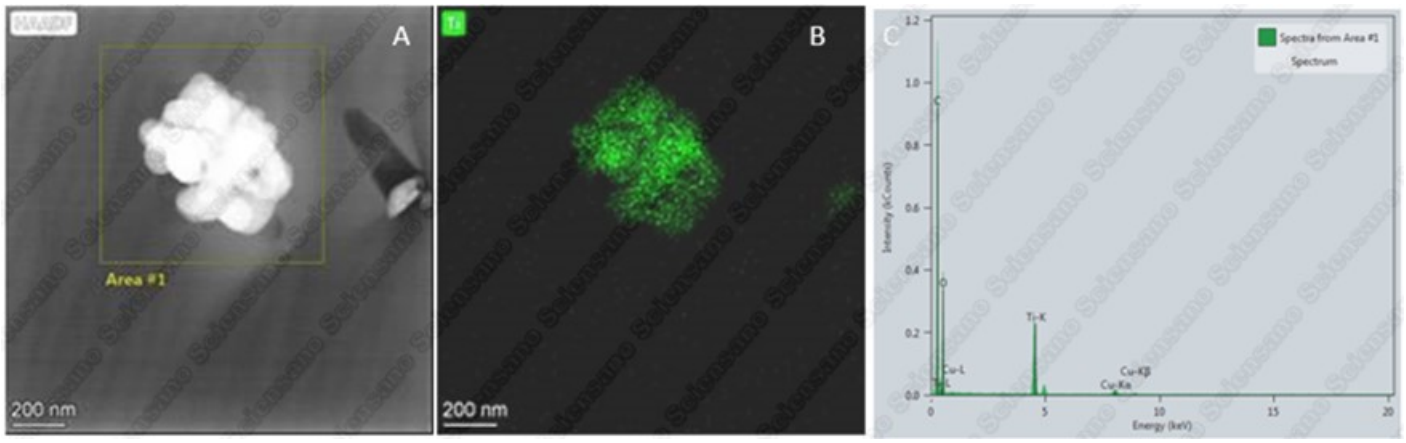

Figure 42 (A) HAADF-STEM image after analysis combined with (B) EDX spectral image of Ti and (C) EDX spectrum of the area indicated in A, demonstating that the particles found in the polyester fibers of sample T17C are TiO_2 particles.

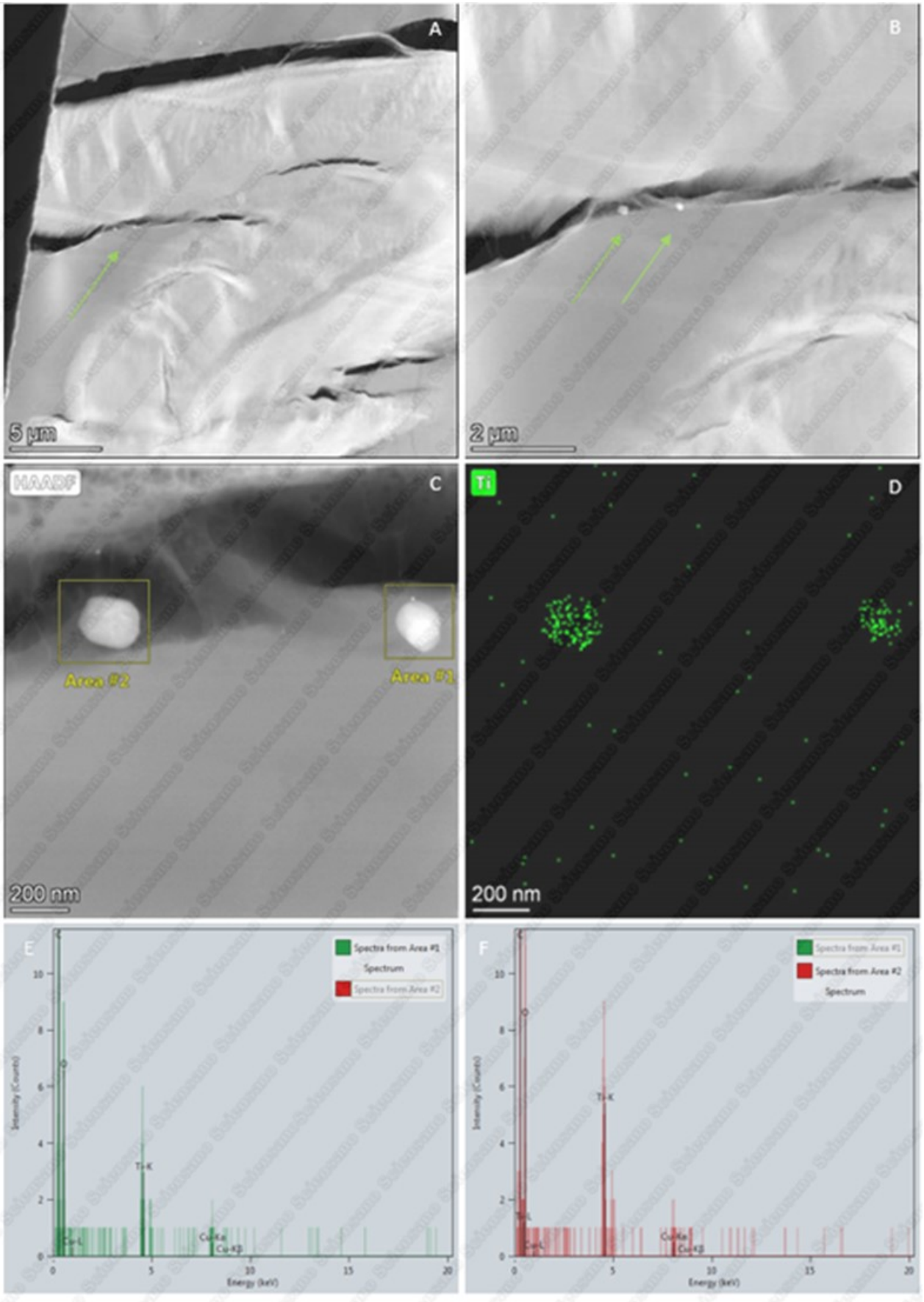

Figure 43 Selected HAADF-STEM images at (A) low, (B) intermediate and (C) high magnifications of the edge of a coton fiber containing nanoparticles (arrow), and corresponding EDX results with (C) the STEM image after analysis, (D) the spectral image of Ti and (E) and (F) the spectrum of the regions indicated in C. Two very small particles can be observed on the STEM image shown in C. These are analysed in Figure 44 and Figure 45.

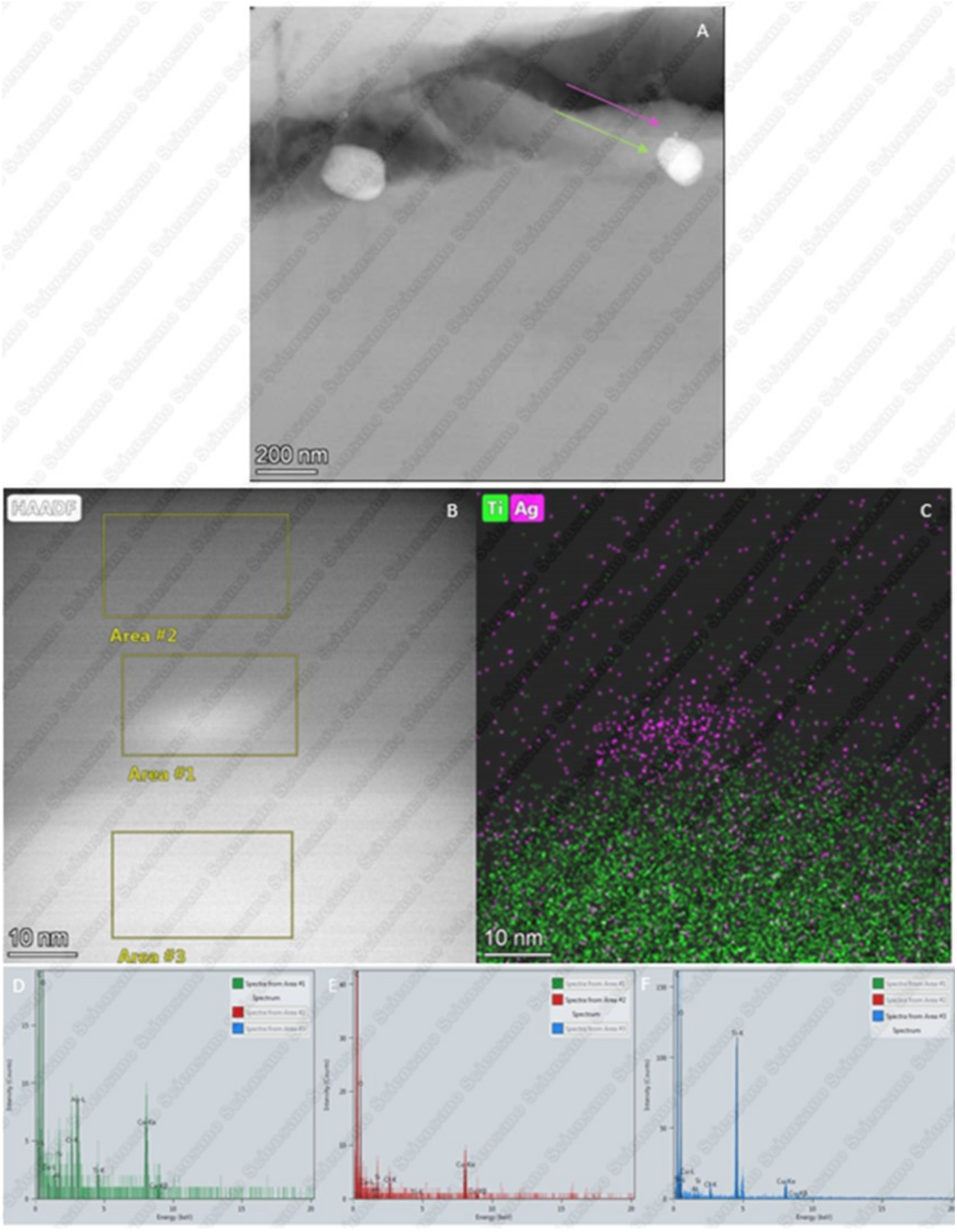

Figure 44 (A) Selected HAADF-STEM image of the edge of a coton fiber containing nanoparticles, and corresponding EDX results of region indicated in A (arrows) with (B) the STEM image after analysis, (C) the spectral image of Ti and Ag, and (D), (E) and (F) the spectra of the regions indicated in B.

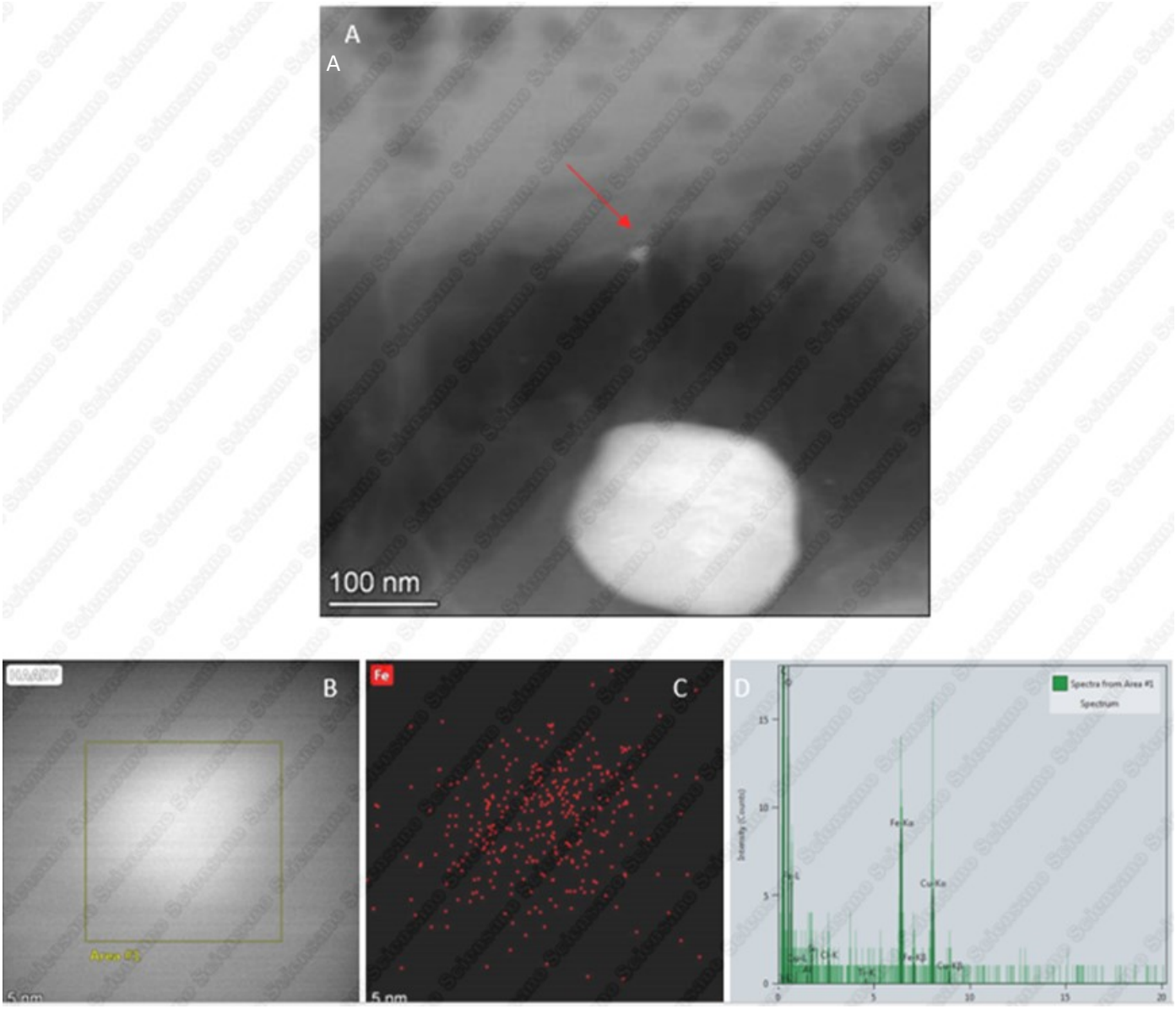

Figure 45 (A) Selected HAADF-STEM image of the edge of a coton fiber containing nanoparticles, and corresponding EDX results of region indicated in A (arrow) with (B) the STEM image after analysis, (C) the spectral image of Fe, and (D), the spectrum of the regions indicated in B.

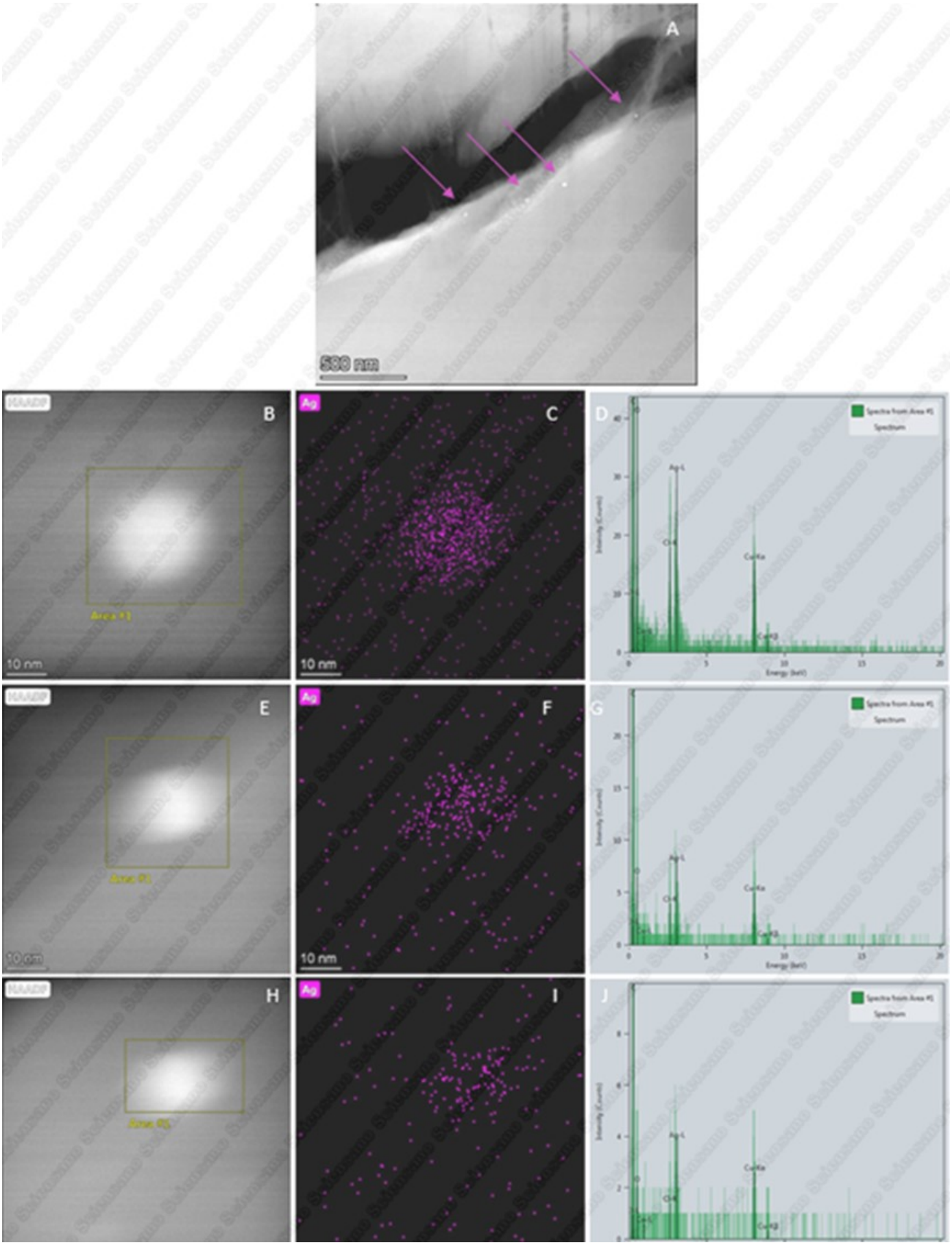

Figure 46 (A) Selected HAADF-STEM image of the edge of a coton fiber containing nanoparticles (arrows), and corresponding EDX results for three particles with (B,E,H) the STEM image after analysis, (C,F,I) the spectral images of Ag and (D, G, J) the spectra of the regions indicated in B, E, and H respectively.

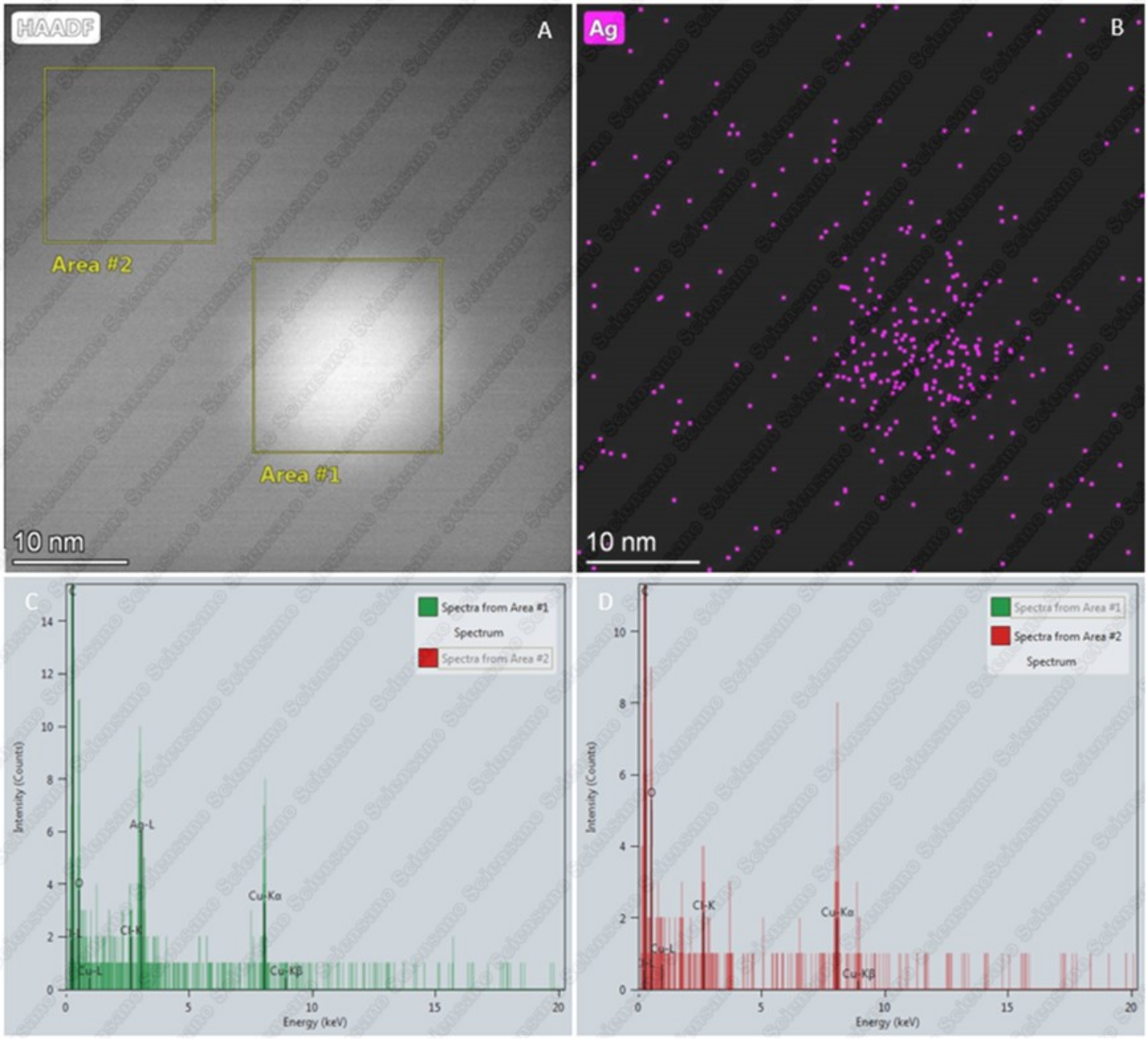

Figure 47 EDX results for the 4th particle indicated in Figure 46 with (A) the STEM image after analysis, (B) the spectral image of Ag, (C, D) the spectra of the regions indicated A. Because no silver signal was detected in the background (area 2), it is shown that the silver signal is measured only where the particle is located (area 1).

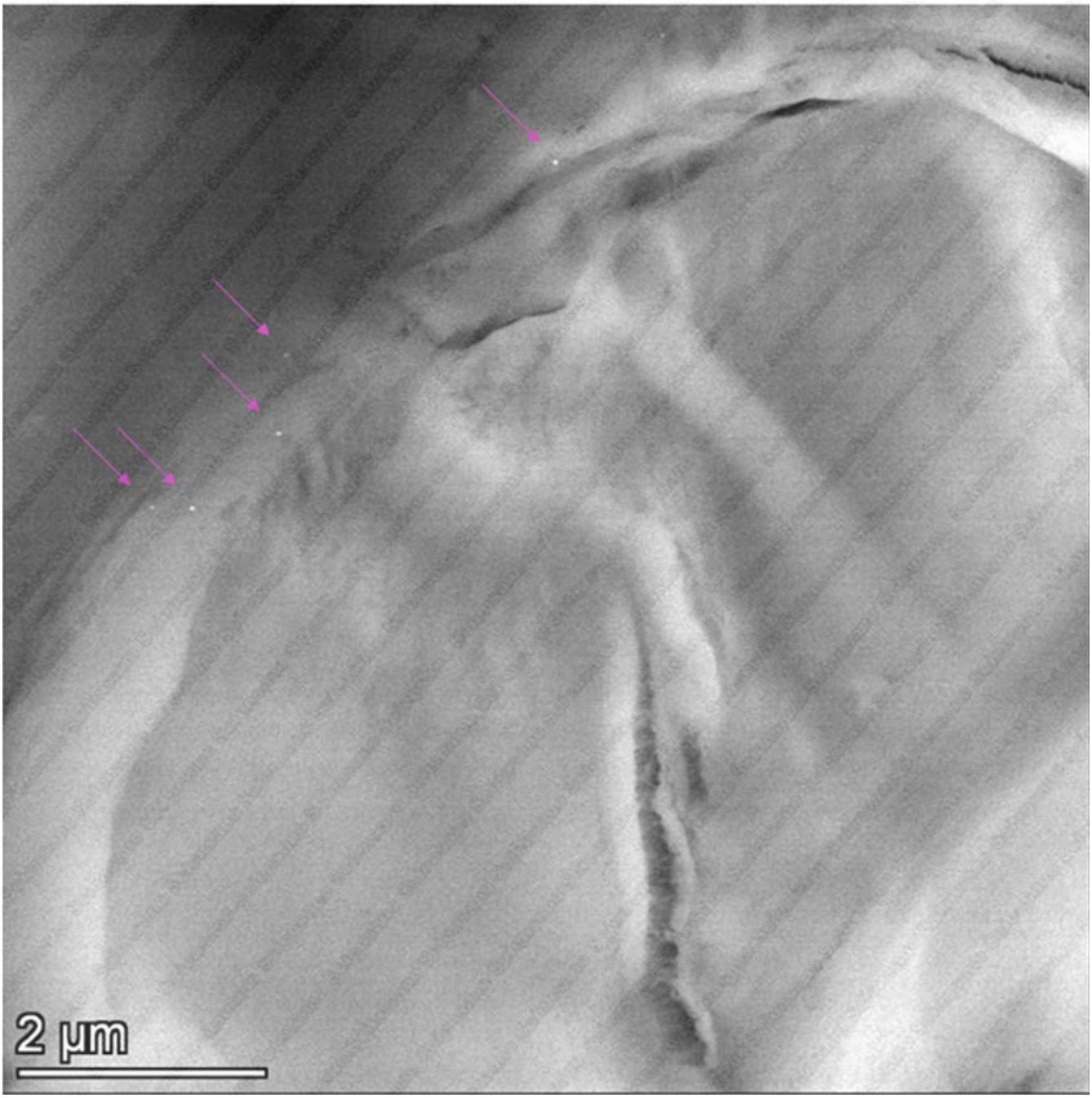

Figure 48 (A) Selected HAADF-STEM image of the edge of a coton fiber containing nanoparticles (arrows)

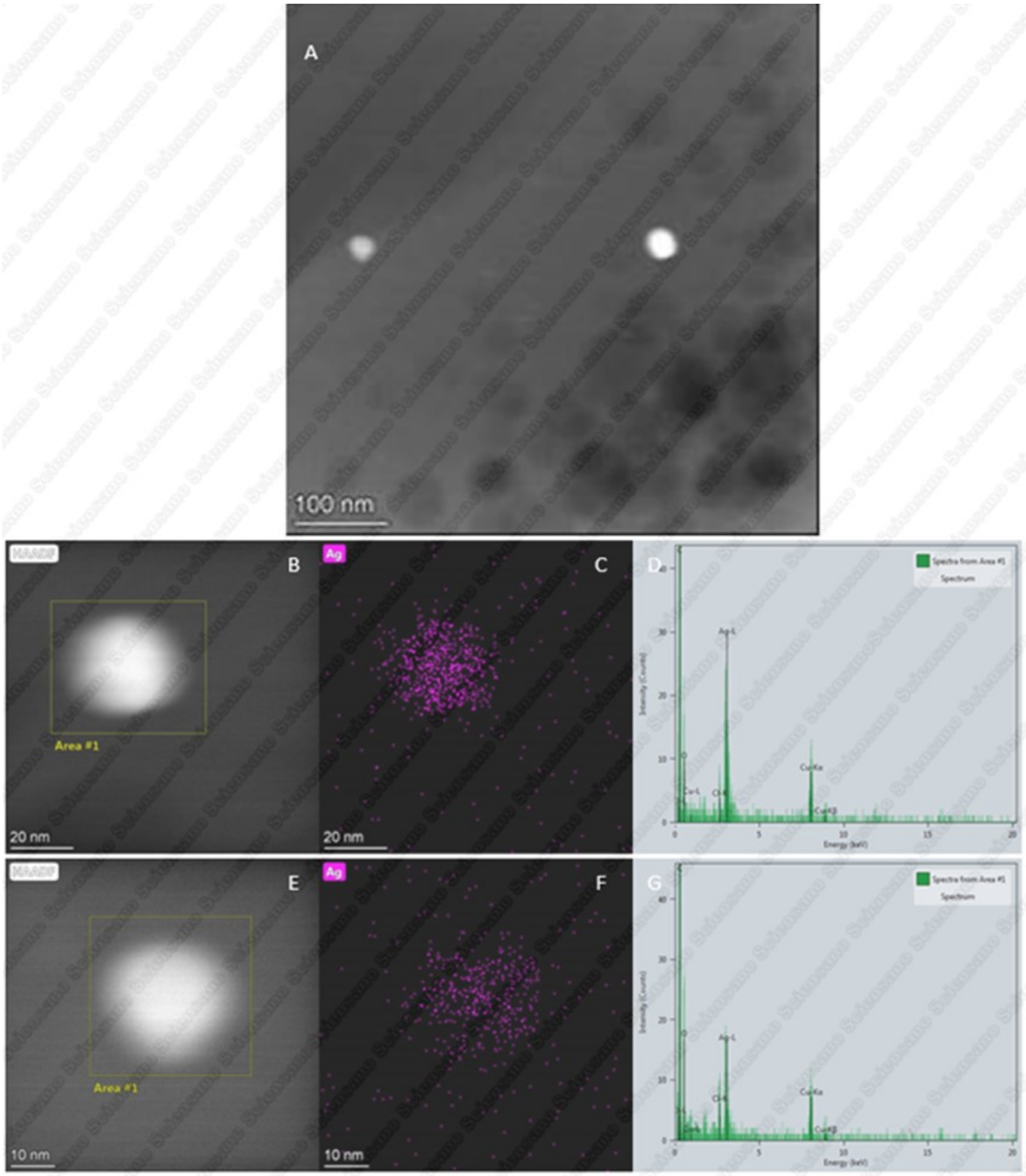

Figure 49 (A) Selected HAADF-STEM image of the edge of a coton fiber containing nanoparticles (magnified image of Figure 48), and corresponding EDX results with (B,E,) the STEM image after analysis, (C,F) the spectral images of Ag and (D, G) the spectra of the regions indicated in B, and E, respectively.

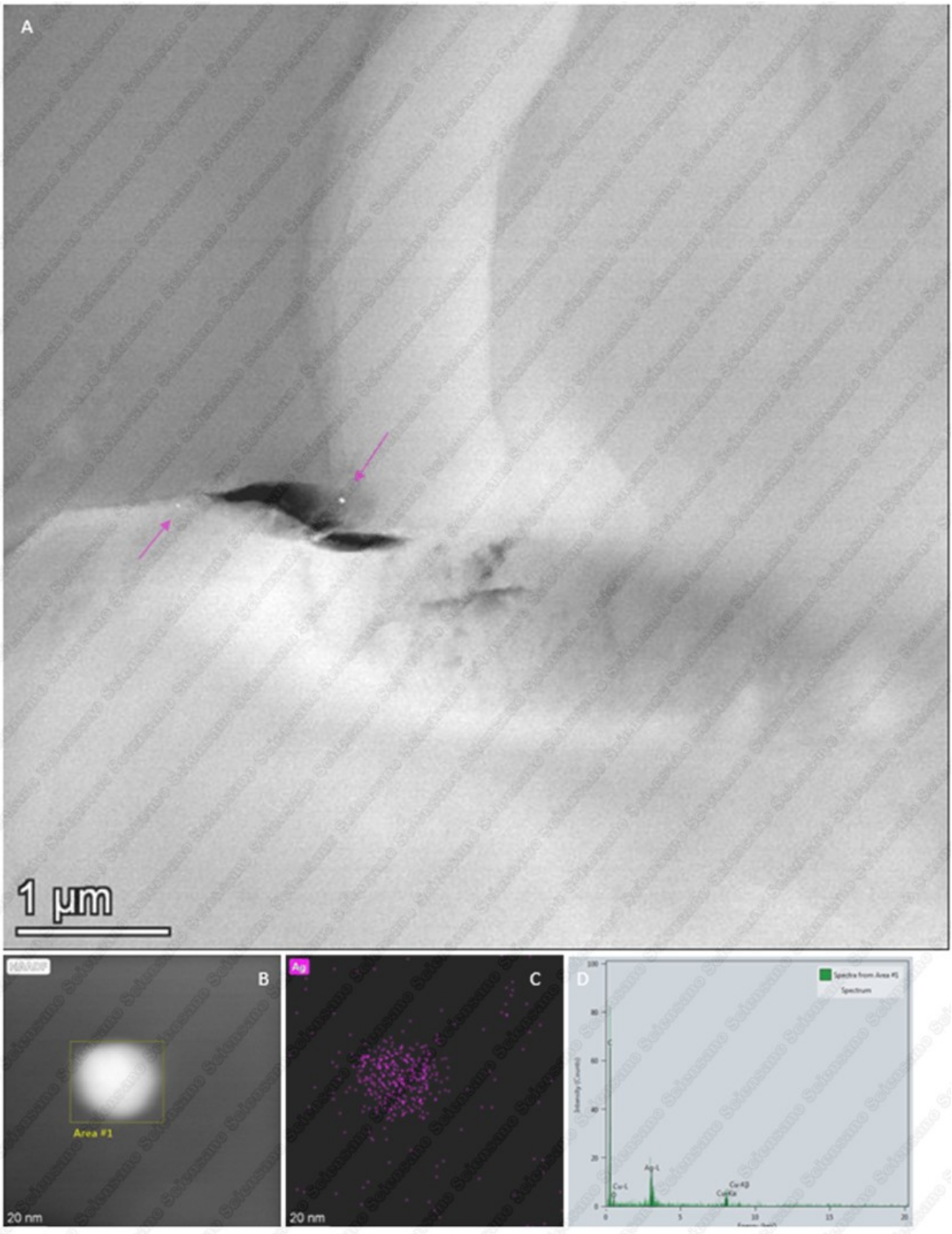

Figure 50 (A) Selected HAADF-STEM image of the edge of a coton fiber containing nanoparticles (arrows) and corresponding EDX results with (B) the STEM image after analysis, (C) the spectral image of Ag and (D) the spectrum of the region indicated in B, respectively.

	Receiver of the report	**Realized by**
Name	**This work was realized in the framework of the AgMask project**	**Unit Electron Microscopy** Service Trace Elements and nanomaterials Sciensano
E-mail		X
Telephone		X
Address		X
Zip Code		X
City		Brussels
Country		Belgium
Other contacts		**Sample preparation:** **Specimen preparartion:** **TEM imaging:** **Image analysis:** **Data analysis:** **Reporting:** **Undersigned by** X, X

References

(1) Mast, J.; Verleysen, E.; De Temmerman, P.-J. Physical Characterization of Nanomaterials in Dispersion by Transmission Electron Microsco-Py in a Regulatory Framework. In *Electron Microscopy of Materials*; Francis, L. D., Mayoral, A., Arenal, R., Eds.; Springer International Publishing AG: Cham, Switzerland, 2014.

(2) Verleysen, E.; Wagner, T.; Lipinski, H.-G.; Kägi, R.; Koeber, R.; Boix-Sanfeliu, A.; De Temmerman, P.-J.; Mast, J. Evaluation of a TEM Based Approach for Size Measurement of Particulate (Nano) Materials. *Materials* **2019**, *12* (14), 2274.

(3) Gashti, M. P.; Alimohammadi, F.; Song, G.; Kiumarsi, A. Characterization of Nanocomposite Coatings on Textiles: A Brief Review on Microscopic Technology. *Current Microscopy Contributions to Advances in Science and Technology* **2012**, *2*, 1424–1437.

(4) Rodenburg, J. M.; Macak, E. B. Optimising the Resolution of TEM/STEM with the Electron Ronchigram. *Microscopy and Analysis* **2002**, *90*, 3.

(5) Pennycook, S. J.; David, B.; Williams, C. B. Transmission Electron Microscopy: A Textbook for Materials Science. *Microscopy and Microanalysis* **2010**, *16* (1), 111.

(6) ISO29301. Microbeam Analysis - Analytical Electron Microscopy - Methods for Calibrating Image Magnification by Using Reference Materials with Periodic Structures. **2017**.

(7) EFSA. Guidance on the Preparation and Presentation of an Application for Authorisation of a Novel Food. *EFSA Journal 2016* **2016**, 24. https://doi.org/10.2903/j.efsa.2016.

(8) EFSA. Scientific Opinion: Guidance on the Risk Assessment of the Application of Nanoscience and Nanotechnologies in the Food and Feed Chain. *EFSA Journal* **2011**, *9* (5), 2140.

(9) SCENIHR. Scientific Committee on Emerging and Newly Identified Health Risks. **2009**.

(10) OECD. *Preliminary Guidance Notes on Sample Preparation and Dosimetry for the Safety Testing of Manufactured Nanomaterials*; 2010.

(11) OECD. *Guidance Manual for the Testing of Manufactured Nanomaterials: OECD Sponsorship Programme: First Revision*; 2010.

(12) Barrett, P. J. The Shape of Rock Particles, a Critical Review. *Sedimentology* **1980**, *27* (3), 291–303. https://doi.org/10.1111/j.1365-3091.1980.tb01179.x.

(13) Munoz-Marmol, M.; Crespo, J.; Fritts, M. J.; Maojo, V. Towards the Taxonomic Categorization and Recognition of Nanoparticle Shapes. *Nanomedicine* **2015**, *11* (2), 457–465. https://doi.org/10.1016/j.nano.2014.07.006 S1549-9634(14)00416-X [pii].

(14) Lopez, O.; Lopez-Iglesias, C.; Cocera, M.; Walther, P.; Parra, J. L.; De La Maza, A. Influence of Chemical and Freezing Fixation Methods in the Freeze-Fracture of Stratum Corneum. *J Struct Biol* **2004**, *146* (3), 302–309. https://doi.org/10.1016/j.jsb.2004.01.003 S1047847704000048 [pii].